

The Development of Magnetic Field Line Wander by Plasma Turbulence

GREGORY G. HOWES and SOFIANE BOUROUAINE

Department of Physics and Astronomy, University of Iowa, Iowa City IA 54224, USA

(Received ?; revised ?; accepted ?. - To be entered by editorial office)

Plasma turbulence occurs ubiquitously in space and astrophysical plasmas, mediating the nonlinear transfer of energy from large-scale electromagnetic fields and plasma flows to small scales at which the energy may be ultimately converted to plasma heat. But plasma turbulence also generically leads to a tangling of the magnetic field that threads through the plasma. The resulting wander of the magnetic field lines may significantly impact a number of important physical processes, including the propagation of cosmic rays and energetic particles, confinement in magnetic fusion devices, and the fundamental processes of turbulence, magnetic reconnection, and particle acceleration. The various potential impacts of magnetic field line wander are reviewed in detail, and a number of important theoretical considerations are identified that may influence the development and saturation of magnetic field line wander in astrophysical plasma turbulence. The results of nonlinear gyrokinetic simulations of kinetic Alfvén wave turbulence of sub-ion length scales are evaluated to understand the development and saturation of the turbulent magnetic energy spectrum and of the magnetic field line wander. It is found that turbulent space and astrophysical plasmas are generally expected to contain a stochastic magnetic field due to the tangling of the field by strong plasma turbulence. Future work will explore how the saturated magnetic field line wander varies as a function of the amplitude of the plasma turbulence and the ratio of the thermal to magnetic pressure, known as the plasma beta.

PACS codes:

1. Introduction

Turbulence remains one of the great unsolved problems of classical physics. Throughout the universe, from distant galaxy clusters to our own heliosphere, 99% of baryonic matter occurs in the plasma state, and these plasmas are nearly always found to be magnetized and turbulent. On the frontier of plasma physics research is the effort to understand how turbulence affects the evolution of any system in which it arises, from terrestrial settings to distant regions of the universe. Plasma turbulence mediates the conversion of the energy of plasma flows and magnetic fields at large scales to plasma heat, or other forms of particle energization. Turbulence may also be a key ingredient in the acceleration of high energy particles at collisionless shocks, and magnetic irregularities caused by turbulence affect the propagation of energetic particles, such as cosmic rays in the Galaxy and solar energetic particles in the heliosphere. The physics of magnetic reconnection may be fundamentally altered in a turbulent medium. Turbulence enhances the loss of angular momentum from accretion disk plasmas, enabling the fueling of black holes and other compact objects. In terrestrial laboratories, turbulence limits the efficiency of proposed

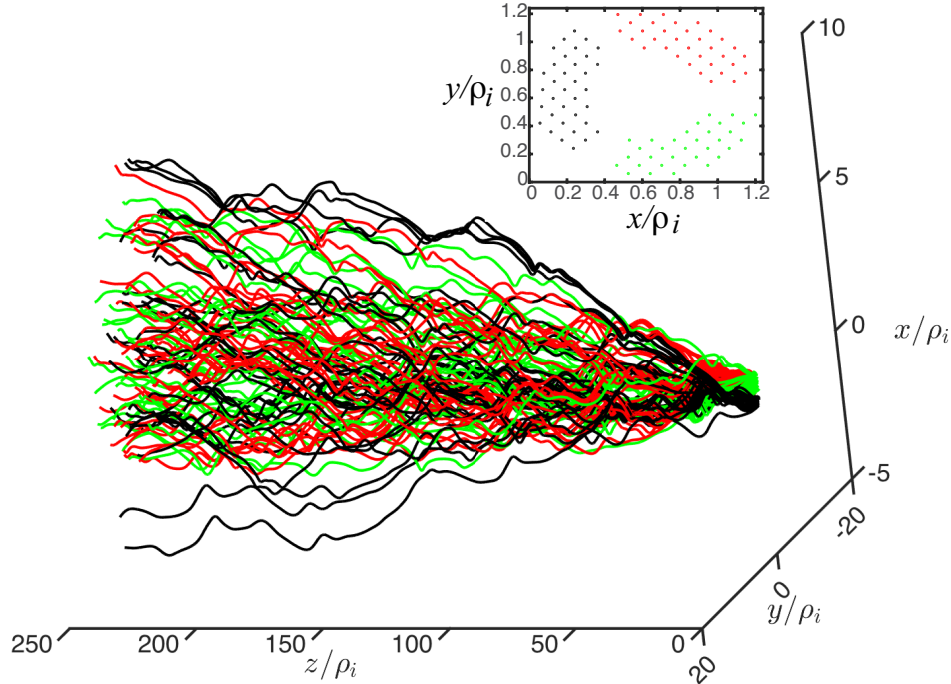


FIGURE 1. Three-dimensional plot of the spreading and tangling of magnetic field lines in a driven, nonlinear gyrokinetic simulation of plasma turbulence relevant to the solar wind. Field lines within four small regions at $z = 0$ are colored red, green, blue, and black. From an initially straight magnetic field, continually driven turbulence, possibly in combination with magnetic reconnection, leads to a stochastically tangled magnetic field. Note the scale of the z -axis is compressed in this plot, so the domain is, in fact, highly elongated.

magnetically confined fusion devices by enhancing the transport of heat and particles across the confining magnetic field.

Although studies of astrophysical turbulence generally focus on how turbulence mediates the conversion of energy from one form to another, plasma turbulence also naturally generates a tangled magnetic field. For example, consider a quiescent, incompressible magnetohydrodynamic (MHD) plasma embedded with a straight and uniform magnetic field. If one drives finite-amplitude Alfvén waves in both directions along that magnetic field, nonlinear interactions among those counterpropagating Alfvén waves will lead to a turbulent cascade of fluctuation energy to small scales (Kraichnan 1965; Similon & Sudan 1989; Sridhar & Goldreich 1994; Goldreich & Sridhar 1995; Maron & Goldreich 2001; Howes *et al.* 2012; Howes & Nielson 2013; Nielson *et al.* 2013; Howes *et al.* 2013; Drake *et al.* 2013). In the process, the magnetic field becomes increasingly tangled, taking on a stochastic appearance, as shown by the rendering of magnetic field lines from a driven, gyrokinetic simulation of plasma turbulence in figure 1. Here, magnetic field lines passing through four small regions at $z = 0$ are given distinct colors. As the field lines are followed through the simulation domain, they spread out and become increasingly tangled up with field lines initially from other regions of the plasma. This phenomenon of *magnetic field line wander* arises due to the nonlinear interactions that mediate the turbulent cascade of energy to small scales, likely in combination with the process of magnetic reconnection.

The inevitable wandering of the magnetic field in turbulent plasmas affects a number of other physical processes, with important unanswered questions regarding its impact on energetic particle propagation in astrophysical and fusion plasmas, the cascade of energy in plasma turbulence, particle acceleration, and magnetic reconnection. Most of the existing studies that attempt to assess the effect of magnetic field line wander on other physical processes, as reviewed below in Section 2, have used a turbulent magnetic field derived from a simplified model or other analytical prescription rather than a turbulent magnetic field generated by direct numerical simulations. Here we advocate a more fundamental approach, using direct numerical simulations to develop a quantitative understanding of how a magnetic field becomes tangled in plasma turbulence as a function of the parameters of the plasma and the turbulence. Theoretical considerations of the tangling of a magnetic field in plasma turbulence are presented in Section 3, including the fundamental parameters upon which the development of magnetic field line wander is likely to depend. Finally, we present some initial quantitative results on the development of magnetic stochasticity and the separation of field lines using nonlinear gyrokinetic simulations that accurately resolve the kinetic microphysics of collisionless magnetic reconnection.

2. Impact of Magnetic Field Line Wander

Magnetic field line wander arising from plasma turbulence impacts important plasma physics processes that govern the evolution of a wide range of important space, astrophysical, and laboratory plasma systems. We review below previous investigations of how the wandering of the magnetic field affects the propagation of energetic particles in astrophysical and fusion plasmas, the cascade of energy in plasma turbulence, the acceleration of particles at collisionless shocks, and the physics of magnetic reconnection.

2.1. Propagation of Cosmic Rays and Energetic Particles

The attempt to understand and predict the propagation of cosmic rays through the interplanetary and interstellar magnetic fields has been a major driver of research into the effect of turbulence on the tangling of the magnetic field. In a seminal early paper, Jokipii (Jokipii 1966) performed the first detailed quasilinear statistical calculation of the motion of charged particles in a spatially random magnetic field, establishing a quantitative connection to the turbulent power spectrum of magnetic field fluctuations. Subsequent work conceptually explained the observed spreading of solar energetic particles from an active region over 180° in solar longitude as a consequence of a magnetic-field-line random walk due to turbulent magnetic field fluctuations (Jokipii & Parker 1968).

The scattering and acceleration of cosmic rays by a spectrum of Alfvén waves with strictly parallel wavenumbers was treated analytically by Schlickeiser (Schlickeiser 1989), and was later extended to include the interaction with fast-mode waves in a low beta plasma (Schlickeiser & Miller 1998). A nonlinear diffusion theory of the stochastic wandering of magnetic field lines, developed by Matthaeus *et al.* (Matthaeus *et al.* 1995), lead to the expectation of diffusive field line wandering in the perpendicular direction.

By the mid-1990s, numerical modeling of the wandering of magnetic field lines began to be widely used, including test particle calculations of energetic particle transport along those turbulent magnetic fields. These efforts require, as input, a model of the spectrum of magnetic fluctuations generated by the plasma turbulence, and a wide variety of such turbulent magnetic field models have been used. Sophisticated numerical field-line following algorithms and complementary analytical approaches have been used to study realizations of slab turbulence models with $\delta\mathbf{B}(z)$ (Schlickeiser 1989; Shalchi & Kourakis

2007*a,b*; Shalchi 2010*b*), 2D turbulence models with $\delta\mathbf{B}(x, y)$ (Shalchi & Kourakis 2007*a,b*; Guest & Shalchi 2012), composite models including slab plus 2D components with $\delta\mathbf{B} = \delta\mathbf{B}(z) + \delta\mathbf{B}(x, y)$ (Bieber *et al.* 1996; Giacalone & Jokipii 1999; Shalchi & Kourakis 2007*a,b*; Qin & Shalchi 2013), and full 3D models with $\delta\mathbf{B}(x, y, z)$, including both isotropic (Zimbardo *et al.* 1995; Giacalone & Jokipii 1999; Ragot 2011; Shalchi 2010*a*) and anisotropic distributions of magnetic fluctuations (Chandran 2000; Zimbardo *et al.* 2000, 2006; Shalchi & Kolly 2013; Ruffolo & Matthaeus 2013).

These various investigations, conducted by a wide range of researchers, have often found conflicting results. The mean square displacement $\langle(\delta r)^2\rangle$ between two magnetic field lines, as they are followed along the magnetic field line a distance l , is often modeled by the power-law form

$$\langle(\delta r)^2\rangle \propto |l|^p. \quad (2.1)$$

For different turbulent magnetic field models, or even a variation of the parameters within a single model, the resulting magnetic field line wandering is sometimes found to be sub-diffusive ($p < 1$) and other times found to be super-diffusive ($p > 1$), and yet other studies recover a standard diffusive behavior ($p = 1$). Based on a broad reading of the literature, the results of the analytical and numerical modeling appear to be rather sensitive to the parameters and properties of the turbulence model chosen. For example, analytical modeling of anisotropic 3D turbulence (with $k_\perp \gg k_\parallel$) suggests the field line wandering is diffusive ($p = 1$) (Shalchi & Kolly 2013), in contrast to the anomalous diffusion ($p \neq 1$) often found using other turbulent models. At present, the wandering of magnetic field lines, and its impact on the propagation of energetic particles, remains an active area of research.

Improved modeling of the propagation of energetic particles in turbulent magnetic fields can have a significant impact on our technological infrastructure, with serious implications for national security. Our society is increasingly dependent on space-borne assets, such as GPS navigation and communication satellites, so the prediction of severe space weather events in near-Earth space has become critically important for the protection of these assets. Solar energetic particle (SEP) events, in which a violent event on the surface of the sun spews high-energy electrons and protons into the heliosphere, represent a threat to both robotic and human assets in space. This prompts an urgent need to develop the ability to predict whether high-energy particles from a particular SEP event will reach the position of a potentially susceptible spacecraft. A predictive capability requires understanding how the SEP particles propagate through the turbulent interplanetary magnetic field. For example, on 3 NOV 2011, an SEP event erupted on the far side of the solar surface, spewing out energetic protons and electrons that were measured at the STEREO A, SOHO, and STEREO B spacecraft, covering more than 200° of solar longitude (Richardson *et al.* 2014). This wide longitudinal spread of significant SEP particle fluxes is not satisfactorily predicted by existing models of SEP propagation. An improved understanding of the magnetic field line wander in the turbulent interplanetary magnetic field, as a function of the plasma and turbulence parameters, is necessary to develop a reliable predictive capability.

In addition to studies of energetic particle propagation, thermal conduction in astrophysical plasmas, such as that occurring in galaxy-cluster cooling flows, has also been found to be strongly affected by a stochastic magnetic field (Chandran & Cowley 1998).

2.2. Magnetic Confinement Fusion

Coincident with the earliest studies on the propagation of energetic particles in space and astrophysical plasmas were complementary studies of anomalous electron heat transport

in tokamaks of the magnetic confinement fusion program. In tokamak plasmas, gradient-driven instabilities generate turbulent fluctuations in the confining magnetic field. It has been proposed that the distortion of magnetic flux tubes as they are mapped along the turbulent confining magnetic field leads to a destruction of the magnetic flux surfaces (Rosenbluth *et al.* 1966; Filonenko *et al.* 1967) that prevent radial mixing of hot central plasma with cold exterior plasma. It was recognized that collisional diffusion is unable to account for all of the electron heat transport measured in experiments, and that magnetic field line wander could potentially explain the additional, “anomalous” transport. Further work quantitatively estimated the diffusion in collisional and collisionless regimes, suggesting that fluctuations of sufficient amplitude, caused by microinstabilities at the scale of the ion gyroradius, would consistently explain both the stochastic nature of the magnetic field and the observed electron heat transport (Rechester & Rosenbluth 1978).

Exploring the role of magnetic field line wander in enhancing electron heat transport in a tokamak plasma has continued over the years using analytical calculations and test particle modeling, and with the comparison of these results to experimental measurements (Galeev & Zeleny 1981; Krommes *et al.* 1983; Haas & Thyagaraja 1986; Laval 1993; Spatschek 2008). Recent advancements in the direct numerical simulation of weakly collisional plasma turbulence using nonlinear gyrokinetic simulations (Pueschel *et al.* 2008; Nevins *et al.* 2011; Wang *et al.* 2011; Hatch *et al.* 2012, 2013) and other direct numerical approaches (del-Castillo-Negrete & Blazevski 2014, 2016) have enabled breakthrough studies of the cause of magnetic field line wander and its impact on confinement in fusion plasmas. Under fusion-relevant plasma conditions, gyrokinetic simulations showed that the magnetic field indeed rapidly becomes stochastic through gradient-instability-driven turbulence, but that this stochasticity does not always produce a significant enhancement in the electron heat flux (Nevins *et al.* 2011). The development of stochasticity appears to arise through nonlinear interactions among overlapping magnetic islands (Wang *et al.* 2011), supporting an idea proposed in early studies based on analytical considerations (Rechester & Rosenbluth 1978). By focusing on the properties of the dominant turbulent modes in ion-temperature-gradient and trapped-electron-mode instability driven turbulence, this overlapping of magnetic islands arises through the nonlinear transfer of energy from the unstable ballooning modes of odd parity to stable tearing modes of even parity (Hatch *et al.* 2012, 2013).

2.3. The Cascade of Energy in Plasma Turbulence

It has been suggested that one can view the the cascade of energy to small scales in magnetized plasma turbulence as due to the distortion of the perpendicular structure of Alfvén wavepackets as they propagating along a wandering, turbulent magnetic field (Similon & Sudan 1989), and this concept has been demonstrated numerically (Maron & Goldreich 2001). An illustration of the distortion of a wavepacket with an initially circular cross section perpendicular to the equilibrium magnetic field from a nonlinear gyrokinetic simulation of plasma turbulence is presented in figure 2. Recent work has adopted this framework to interpret current sheet formation in coronal loops (Rappazzo & Parker 2013), the nonlinear transfer of energy to smaller scale Alfvén waves in basic laboratory experiments of plasma turbulence (Howes *et al.* 2012; Howes & Nielson 2013; Nielson *et al.* 2013; Howes *et al.* 2013; Drake *et al.* 2013), and the evolution of magnetic flux surfaces in 3D reduced MHD simulations (Servidio *et al.* 2014).

Looking at this problem in more detail, the nonlinear physics underlying the turbulent cascade of energy from large to small scales is often described in Fourier space, where a nonlinear three-wave coupling mechanism has been identified that leads to a secu-

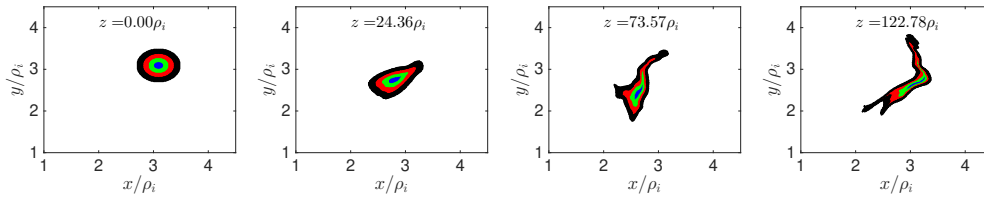


FIGURE 2. The distortion of a circular wavepacket as it propagates along the wandering magnetic field in a nonlinear gyrokinetic simulation of plasma turbulence.

lar transfer of energy to modes with higher perpendicular wavenumber (Shebalin *et al.* 1983; Sridhar & Goldreich 1994; Montgomery & Matthaeus 1995; Ng & Bhattacharjee 1996; Galtier *et al.* 2000; Howes & Nielson 2013), resulting in an anisotropic cascade of energy in wavevector space. But the physical manifestation of the $k_{\parallel} = 0$ mode that mediates this resonant three-wave interaction is obscured by the use of the Fourier (plane-wave) decomposition. An analytical calculation modeling interactions between localized Alfvén wavepackets demonstrated that wavepackets involving a $k_{\parallel} = 0$ component will lead to this lowest-order three-wave nonlinear coupling (Ng & Bhattacharjee 1996), and this mechanism has been demonstrated using laboratory experiments (Howes *et al.* 2012, 2013; Drake *et al.* 2013). Physically, the $k_{\parallel} = 0$ component of a wavepacket represents a shear in the magnetic field, as depicted in figure 3. Investigation of the propagation of Alfvén waves in a wandering magnetic field demonstrates that the cascade of energy to small scales is represented in physical space (as opposed to Fourier space) as a shearing of the perpendicular structure of an Alfvén wave as it propagates along a wandering magnetic field, as depicted in figure 3(c) and (f). Thus, exploring the complementary picture of the plasma turbulent cascade as the distortion of Alfvén waves as they propagate along a wandering magnetic field may yield fresh insights into the nature of plasma turbulence.

2.4. Particle Acceleration

Models of diffusive shock acceleration at collisionless shocks require irregularities in the upstream magnetic field to return reflected particles back to the shock front repeatedly to achieve significant acceleration (Ragot 2001; Guo & Giacalone 2010, 2013, 2015). The efficiency of such a shock-acceleration mechanism is likely to be dependent on the nature of the upstream magnetic field irregularities, but existing investigations of these particle acceleration mechanisms often use unrealistic models of the turbulent plasma, such as slab turbulence with only a one-dimensional variation of the turbulent field, $\delta\mathbf{B}(z)$ (Guo & Giacalone 2010). The development of a new empirical model of magnetic field line wander based on direct numerical simulations of plasma turbulence will enable more realistic modeling of the diffusive acceleration mechanism at collisionless shocks.

2.5. Magnetic Reconnection

It has been proposed theoretically that magnetic field line wander can alter the physics of magnetic reconnection when the upstream plasma is turbulent (Lazarian & Vishniac 1999), increasing the rate of reconnection and the thickness of the current sheets in the turbulent medium (Vishniac *et al.* 2012). Numerical simulations have played a key role in bearing out these ideas (Kowal *et al.* 2009, 2012). It has also been claimed that exponential field line separation in turbulent plasmas will lead to reconnection even in the absence of intense current sheets (Boozer 2014). It has been shown that stochasticity of the magnetic field in MHD turbulence simulations degrades the usual notion of

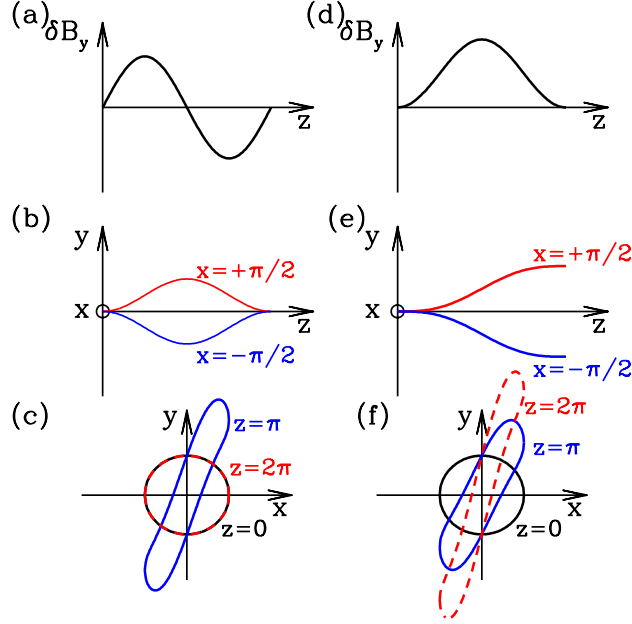


FIGURE 3. Distortion of a magnetic flux tube in the perpendicular (x, y) plane due to wandering of the magnetic field. (a) Magnetic field fluctuation δB_y contains no $k_z = 0$ component. (b) 3D tracing of magnetic field lines due to the magnetic fluctuation in (a) at positions $x = +\pi/2$ (red) and $x = -\pi/2$ (blue). The oscillating shear causes the magnetic field to become sheared and then subsequently to “unshear.” (c) The distortion of an Alfvén wave with an initially circular perpendicular structure (black) as it propagates along the wandering magnetic field. (d) For the case of a magnetic field fluctuation δB_y with a nonzero $k_z = 0$ component, the (e) 3D magnetic field has a monotonic shear, leading to (f) the permanent distortion (red) of an initially circular Alfvén wave structure (black).

flux-freezing in an MHD plasma, potentially explaining fast reconnection of large-scale structures at MHD scales (Eyink *et al.* 2013). More recently, numerical simulations have been used to explore how breaking field line connectivity by stochasticity of the magnetic field can be a mechanism for fast reconnection (Huang *et al.* 2014). The properties of the turbulent upstream magnetic fields very likely influence how the reconnection mechanism is modified, so an improved model of magnetic field line wander in plasma turbulence will contribute to progress in the understanding of magnetic reconnection under the turbulent conditions of realistic space and astrophysical plasma environments.

3. Theoretical Considerations

This study aims to use direct numerical simulations to illuminate the physical processes influencing the development and saturation of magnetic field line wander in astrophysical plasma turbulence. The ultimate goal is to construct an empirical description of the magnetic field line wander in terms of the fundamental turbulence and plasma parameters. This empirical description can be utilized to describe accurately the properties of the turbulently tangled magnetic field for application to studies of energetic particle transport in astrophysical and laboratory plasmas, the cascade of energy to small scales in

plasma turbulence, the acceleration of particles to high energies by collisionless shocks, and the physics of magnetic reconnection in a turbulent plasma.

3.1. *Improving Our Understanding through Direct Numerical Simulations*

As detailed above, the nature of the magnetic field line wander in previous studies appears to be quite sensitive to the characteristics and parameters of the models describing the turbulent magnetic field. Many of the models of the turbulent magnetic field used in the literature exploring the phenomenon of magnetic field line wander and its implications are severely outdated, being inconsistent with the current understanding of plasma turbulence. Specifically, models employing slab, 2D, composite (slab plus 2D), and isotropic distributions of magnetic fluctuations, although more susceptible to theoretical analysis, are at odds with the anisotropic, 3D nature of plasma turbulence that is now well-established through decades of experimental, analytical, and numerical research on magnetized plasma turbulence (Robinson & Rusbridge 1971; Belcher & Davis 1971; Zweben *et al.* 1979; Montgomery & Turner 1981; Shebalin *et al.* 1983; Cho & Vishniac 2000; Maron & Goldreich 2001; Cho & Lazarian 2004, 2009; TenBarge & Howes 2012). Recent direct multi-spacecraft measurements of turbulence in the solar wind confirm this anisotropic nature of the turbulent fluctuations (Sahraoui *et al.* 2010; Narita *et al.* 2011; Roberts *et al.* 2013, 2015).

In addition, the models employed in the studies reviewed above almost universally employ randomly phased magnetic field fluctuations, a characteristic inconsistent with any self-consistent realization of a turbulent magnetic field. Kolmogorov’s Four-fifths Law (Kolmogorov 1941) is an exact statistical formula relating the mean energy dissipation rate to the third-moment of the velocity fluctuations in hydrodynamic turbulence; subsequently, this third-moment approach has been extended for the case of MHD turbulence (Chandrasekhar 1951; Politano & Pouquet 1998; Yousef *et al.* 2007). A spectrum of magnetic fluctuations with random phases yields an average third-moment of zero, because it is the phase correlations among different magnetic fluctuations that are responsible for the nonlinear turbulent cascade of energy. Random-phase models therefore lack some of the inherent attributes of a self-consistently determined turbulent magnetic field (Howes 2015, 2016). It remains an open question whether such correlations will indeed alter the nature of the magnetic field line wander resulting from plasma turbulence, but the apparent sensitivity of the results of previous studies to the characteristics of the magnetic field model suggests that a self-consistent turbulent magnetic field will yield the most well-justified and physically relevant results.

The uncertainty in describing the turbulent magnetic field can be eliminated by using a turbulent magnetic field that is generated self-consistently by direct numerical simulation of the equations governing the turbulent plasma dynamics. Of the studies directly investigating magnetic field line wander reviewed above, only the recent studies of stochastic magnetic field development in fusion plasmas (Pueschel *et al.* 2008; Nevins *et al.* 2011; Wang *et al.* 2011; Hatch *et al.* 2012, 2013) employed direct numerical simulations, specifically using a nonlinear gyrokinetic code. A general approach to understand the development and saturation of the tangled magnetic field in general astrophysical plasma turbulence has not been attempted, and this provides a strong motivation for the present work.

3.2. *The Role of Magnetic Reconnection*

Another important ingredient in understanding how magnetic fields become dynamically tangled by plasma turbulence is the process of magnetic reconnection. Although the impact of pre-existing turbulent magnetic fields on the process of magnetic reconnection

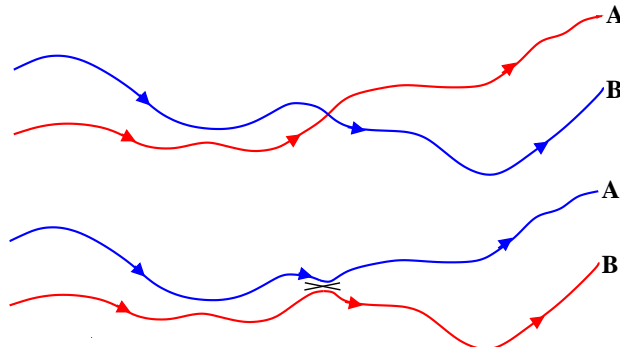


FIGURE 4. Illustration of how magnetic reconnection can instantaneously change the magnetic connectivity in a turbulent plasma, thereby influencing the development of magnetic field line wander.

tion has been examined previously (Lazarian & Vishniac 1999; Kowal *et al.* 2009, 2012; Vishniac *et al.* 2012; Boozer 2014; Huang *et al.* 2014), the investigation of how reconnection mediates the tangling and untangling of magnetic fields in plasma turbulence has not been addressed by any existing study. For example, consider the two turbulent magnetic field lines depicted in figure 4. When a small reconnection event (denoted by the black cross) occurs between the two field lines, the connectivity of those two field lines changes instantaneously. Particles streaming along the red field line from the left end of the plasma, which previously had been connected to point A, will suddenly find themselves magnetically connected instead to point B. An open question is whether the impact of magnetic reconnection on the wandering of magnetic field lines can be described in the framework of a diffusion, or whether this possibility of sudden jumps in connectivity alter the nature of the resulting magnetic field line wander. Direct numerical simulations of the turbulent plasma that resolve the physics of magnetic reconnection, even in the collisionless limit relevant to many space and astrophysical systems of interest, are critical for answering this open question.

3.3. The Turbulent Solar Wind as a Fiducial Example

The turbulent solar wind that pervades our heliosphere represents a fiducial system supporting a broad spectrum of turbulent plasma motions over more than seven orders of magnitude in scale (Kiyani *et al.* 2015). It is also the most thoroughly diagnosed turbulent astrophysical plasma in the universe, thereby providing unique opportunities for confronting any empirical description of magnetic field line wander with direct, *in situ* measurements of the turbulent interplanetary magnetic field. Thus, the solar wind provides an ideal case study for discussing the phenomenon of magnetic field line wander in a turbulent plasma. In addition, the tangling of the magnetic field in the solar wind has important consequences for the propagation of solar energetic particles erupting from violent solar activity, constituting an important space weather hazard for spaceborne human and technological assets. Improving the modeling of the tangled magnetic field in the heliosphere therefore has important societal implications.

Figure 5 presents a diagram of the solar wind magnetic energy wavenumber spectrum—assuming the Taylor hypothesis (Taylor 1938) to convert the spacecraft-frame frequency to a corresponding wavenumber of spatial fluctuations in the super-Alfvénic solar wind (Howes *et al.* 2014; Klein *et al.* 2014)—for near-Earth space at $R \sim 1$ AU. At the largest scales $l > 10^6$ km (lowest wavenumbers) is the *energy containing range* (Matthaeus *et al.* 1994; Tu & Marsch 1995; Bruno & Carbone 2005), populated by large-scale plasma flow

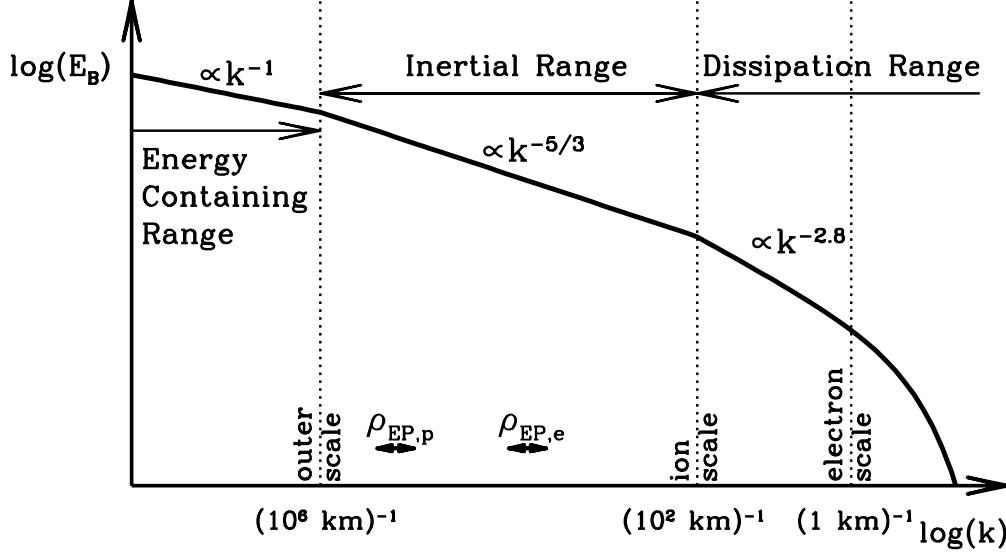


FIGURE 5. Schematic of the magnetic energy wavenumber spectrum in the solar wind, showing the form of the spectrum in the energy containing, inertial, and dissipation ranges. Ranges for the typical Larmor radius scales for protons $\rho_{EP,p}$ and electrons $\rho_{EP,e}$ from Solar Energetic Particle (SEP) events are depicted.

and magnetic field fluctuations. Through nonlinear interactions, these energy containing fluctuations feed their energy into the turbulent cascade at the outer scale, $l \sim 10^6$ km, where the steepening of the magnetic energy spectrum marks the beginning of the turbulent *inertial range* (Tu & Marsch 1995; Bruno & Carbone 2005). Within the inertial range, energy is nonlinearly transferred scale by scale in a self-similar manner, leading to a single power-law spectrum down to the inner scale, which corresponds to one of the characteristic ion kinetic length scales at $l \sim 10^2$ km. At this ion scale, the magnetic energy spectrum breaks once again (Bourouaine *et al.* 2012), marking the transition to the *dissipation range*[†] (Sahraoui *et al.* 2009; Kiyani *et al.* 2009; Alexandrova *et al.* 2009; Chen *et al.* 2010; Sahraoui *et al.* 2010, 2013). Finally, at the characteristic electron length scale of $l \sim 1$ km, the magnetic energy spectrum is often observed to exhibit an exponential roll-off (Alexandrova *et al.* 2012; Sahraoui *et al.* 2013), interpreted to indicate the ultimate termination of the turbulent cascade. Also plotted on figure 5 is a representation of the Larmor radius scales for protons and electrons from Solar Energetic Particle (SEP) events, $\rho_{EP,p}$ and $\rho_{EP,e}$; collisionless wave-particle interactions of energetic particles with the turbulent magnetic fluctuations lead to scattering rates that peak at these Larmor scales. Simulations using the gyrokinetic code **AstroGK** reproduce quantitatively the features of the solar wind magnetic energy spectrum from the middle of the inertial range down to the sub-electron scales (TenBarge *et al.* 2012, 2013).

It is the turbulent magnetic field fluctuations over this broad range of scales that lead to the stochastic character of the magnetic field, so investigating how fluctuations in different scale ranges of this spectrum affect the magnetic field line wandering is an important long-term goal. To accomplish this goal, direct numerical simulations can be used to learn how magnetic field line wander develops and saturates in plasma turbulence.

[†] The name dissipation range is the most commonly used term, although use of this term is *not* intended to imply that the steepening of the spectrum here is necessarily due to dissipation.

3.4. A Model for the Development and Saturation of Magnetic Field Line Wander

Here we propose a novel theoretical picture of the plasma physical processes involved in the development of magnetic field line wander and its saturation. The nonlinear interactions that underlie the turbulent cascade of energy to small scales also lead to a tangling of the magnetic field. In an ideal plasma with no magnetic reconnection, this tangling of the field would continue indefinitely, generating turbulent structures on ever smaller scales, leading to an ever more intricate wandering of the magnetic field. But, once the turbulent structures have reached sufficiently small scales that non-ideal physics breaks the frozen-in condition, magnetic reconnection may ensue, thereby untangling the magnetic field. We propose that the saturation of the magnetic field line wander represents a balance between the nonlinearly-driven tangling and the magnetic-reconnection-mediated untangling, a physical picture that we aim to test thoroughly using direct numerical simulations.

A key observation is that these two mechanisms, nonlinear interactions (turbulence) and magnetic reconnection, depend differently on the fundamental parameters describing the turbulence and the plasma. For example, the physics of magnetic reconnection has a strong dependence on the plasma β , but the physics of the turbulent nonlinear energy transfer appears to have very little dependence on this plasma parameter (Howes & Nielson 2013; Nielson *et al.* 2013; Howes 2015). What is entirely new here, compared to the body of literature on turbulent magnetic field line wander, is that most previous works[†] have completely ignored any role played by magnetic reconnection. From the theoretical picture above—a balance between turbulent tangling and reconnective untangling—we believe that it is inevitable that magnetic reconnection plays an important role in the physics of magnetic field line wander, possibly leading to an important, and as yet unrecognized, dependence on the plasma β . A study based on direct numerical simulations that resolve the kinetic microphysics of magnetic reconnection is likely to break new ground on this important frontier in the study of magnetic field line wander and its implications for many important physical processes in the universe.

Discussions of the tangling of the magnetic field by plasma turbulence often employs the term “stochastic magnetic field” as a generic label for any turbulently tangled magnetic field. Here we reserve the use of the term *stochastic* to cases in which the magnetic field indeed demonstrates a stochastic character, as demonstrated by an appropriate analysis, such as a Poincare recurrence plot (see section 6). We choose to use the term *magnetic field line wander* to refer to the general case when the magnetic field does exhibit a topology in which the separation between two field lines increases (or decreases) as one moves a distance along the field, whether or not the magnetic field exhibits a stochastic character. How the physics of energetic particle propagation in astrophysical plasmas, heat and particle transport in fusion plasmas, magnetic reconnection, and particle acceleration differs when the magnetic field lines merely wander, but are not fully stochastic, is an interesting open question.

3.5. Key Questions

To investigate and characterize the development and saturation of magnetic field line wander in turbulent plasmas, direct numerical simulations provide a valuable tool. Since magnetic reconnection may play an essential role in the physics of the field line tangling, a numerical method that resolves the kinetic microphysics of magnetic reconnection, particularly under the weakly collisional conditions relevant to many turbulent space and astrophysical plasma systems, is essential. This can be supplemented by fluid methods to

[†] With the exception of studies directly focusing on magnetic reconnection.

explore how the nonlinear dynamics at large scales governs the tangling of the magnetic field. Such an approach, maintaining a strong connection to the nonlinear dynamics of plasma turbulence and magnetic reconnection, will enable important new questions about the nature of magnetic field line wander caused by plasma turbulence to be addressed:

- (a) How does magnetic field line wander develop and saturate in plasma turbulence?
- (b) Do the properties of magnetic field line wander depend on the underlying physical mechanism that enables magnetic reconnection (collisionless vs. resistive vs. numerical reconnection)?
- (c) Is magnetic field line wander dominated by the large-scale or small-scale fluctuations of the turbulence?
- (d) Can we construct an empirical description of the magnetic field line wander in terms of the fundamental plasma and turbulence parameters?

3.6. Quantitative Dependence on Fundamental Turbulence and Plasma Parameters

Turbulence in heliospheric and other astrophysical plasmas naturally leads to the tangling of the magnetic field, leading to the development of magnetic field line wander, a property that we would like to characterize quantitatively. To develop a quantitative measure of the wandering of field lines in such a plasma, consider choosing two points on different field lines separated by a distance δr perpendicular to the magnetic field. For these two particular points, one may compute the perpendicular separation between the two field lines in the perpendicular plane as a function of the distance along the magnetic field line l . Computing statistics of this quantity using direct numerical simulations of plasma turbulence enables the development of the quantitative characterization of the magnetic field line wander.

The statistics of this perpendicular separation δr between two magnetic field lines can be quantitatively characterized in terms of a small number of important parameters. First are basic parameters to describe the wandering of field lines away from each other, including the distance traveled along the field line l and the time for which turbulence has been dynamically tangling the field. Next are the dimensionless parameters that describe the turbulence itself. The amplitude, or strength, of the turbulence is characterized by the *nonlinearity parameter*, $\chi = k_{\perp} \delta B_{\perp} / (k_{\parallel} B_0)$ (Goldreich & Sridhar 1995; Howes & Nielson 2013), describing the amplitude of the turbulence at the driving scale (equivalent to the “Kubo” number in some previous studies (Zimbardo *et al.* 2000)). For example, to explore the impact on particle diffusion by the amplitude of turbulent fluctuations, one study computed particle trajectories numerically in a tangled magnetic field consisting of 1000 randomly phased plane-wave modes (Hauff *et al.* 2010), and another study used Ramaty High Energy Solar Spectroscopic Imager (RHESSI) observations of hard X-rays to estimate the magnitude of magnetic field-line diffusion in flaring coronal loops under several assumptions (Bian *et al.* 2011). Both studies found that, in the large Kubo number limit ($\chi \gg 1$), perpendicular diffusion becomes independent of the turbulence spectrum, in agreement with the predictions of percolation theory (Gruzinov *et al.* 1990; Isichenko 1992).

Another key dimensionless parameter is the *isotropic driving wavenumber*, $k_0 \rho_i$ (Howes *et al.* 2008a, 2011), describing the driving scale, or energy injection scale, of the turbulence normalized to the ion Larmor radius, where it is assumed the turbulent fluctuations are isotropic with respect to the direction of the mean magnetic field at this scale[†]. Finally, the key dimensionless parameters that describe the plasma are the ion plasma beta,

[†] The assumption of isotropic driving may be relaxed if physical arguments suggest anisotropic driving, where an appropriate scaling theory for the anisotropic cascade of plasma turbulence can be used to devise a suitable dimensionless parameter to replace $k_0 \rho_i$.

$\beta_i = 8\pi n_0 T_i / B_0^2$, and the ion-to-electron temperature ratio, T_i/T_e . In summary, therefore, we expect that the separation between two magnetic field lines δr as one follows the field lines through the plasma to have a dependence on these fundamental parameters given by $\delta r(l, t, \chi, k_0 \rho_i, \beta_i, T_i/T_e)$.

For the most likely case of saturated turbulence in steady state, where the tangling of the magnetic field by the turbulence and untangling of the field by magnetic reconnection statistically balance, we conjecture that the δr will not depend on time. A reasonable form to seek for the average squared field line separation in a turbulent steady state, $\langle (\delta r)^2 \rangle$, based on the previous analyses reviewed in section 2, can be written

$$\langle (\delta r)^2 \rangle = A l^p. \quad (3.1)$$

Here $A(\chi, k_0 \rho_i, \beta_i, T_i/T_e)$ represents the amplitude of the average spreading of field lines, and we assume the average squared field line separation can be expressed as a power law of the distance along the field line l , given by the exponent $p(\chi, k_0 \rho_i, \beta_i, T_i/T_e)$. The long term goal of this project is to determine empirically forms for A and p that can be used to characterize the magnetic field line wander in terms of the turbulence and plasma parameters.

Although the two turbulence parameters χ and $k_0 \rho_i$ together with the two plasma parameters β_i and T_i/T_e leads to a four dimensional parameter space, the broad range of different turbulence models previously used to explore magnetic field line wander requires a much longer list of possible parameters. The most likely culprit responsible for the many conflicting results found in the literature is the tremendous variation among the different models chosen to describe the turbulent magnetic field. The use of direct numerical simulations of plasma turbulence enables us to eliminate the huge parameter space necessary to describe the plethora of different magnetic field models reviewed in section 2, at the expense of the necessarily limited dynamic range attainable by direct numerical simulations. But we believe that a more physically faithful characterization of the magnetic field line wander in plasma turbulence can be patched together through a judicious use of different simulation models appropriate to different ranges of the turbulent spectrum, as depicted in Figure 5.

4. Code and Description of Turbulence Simulations

The Astrophysical Gyrokinetics Code, or **AstroGK**, described in detail in Numata *et al.* (2010), evolves the perturbed gyroaveraged distribution function $h_s(x, y, z, \lambda, \varepsilon)$ for each species s , the scalar potential φ , parallel vector potential A_{\parallel} , and the parallel magnetic field perturbation δB_{\parallel} according to the gyrokinetic equation and the gyroaveraged Maxwell's equations (Frieman & Chen 1982; Howes *et al.* 2006), where \parallel is along the total local magnetic field $\mathbf{B} = B_0 \hat{\mathbf{z}} + \delta \mathbf{B}$. The velocity space coordinates are $\lambda = v_{\perp}^2/v^2$ and $\varepsilon = v^2/2$. The domain is a periodic box of size $L_{\perp}^2 \times L_z$, elongated along the equilibrium magnetic field, $\mathbf{B}_0 = B_0 \hat{\mathbf{z}}$. Note that, in the gyrokinetic formalism, all quantities may be rescaled to any parallel dimension satisfying $\epsilon \equiv L_{\perp}/L_z \ll 1$. Uniform Maxwellian equilibria for ions (protons) and electrons are used, with the correct mass ratio $m_i/m_e = 1836$. Spatial dimensions (x, y) perpendicular to the equilibrium field are treated pseudospectrally; an upwind finite-difference scheme is used in the parallel direction. Collisions are incorporated using a fully conservative, linearized Landau collision operator that includes energy diffusion and pitch-angle scattering due to electron-electron, ion-ion, and electron-ion collisions (Abel *et al.* 2008; Barnes *et al.* 2009), yielding an isotropic Maxwellian stationary solution.

The simulations presented here are similar to previous nonlinear gyrokinetic simula-

tions used to investigate the physics of the turbulence in the weakly collisional solar wind (Howes *et al.* 2008*b*; Howes *et al.* 2011), in particular the small scale simulations of the kinetic Alfvén wave cascade down to the scales of the electron Larmor radius (TenBarge & Howes 2013; TenBarge *et al.* 2013). We present here results of a simulation of a driven, strongly turbulent kinetic Alfvén wave cascade in a plasma with parameters $\beta_i = 1$ and $T_i/T_e = 1$, where $\beta_i = v_{ti}^2/v_A^2$, v_A is the Alfvén speed, $v_{ti} = \sqrt{2T_i/m_i}$ is the ion thermal speed, and temperature is expressed in units of energy. The simulation domain has dimensions $(n_x, n_y, n_z, n_\lambda, n_\epsilon, n_s) = (64, 64, 32, 32, 16, 2)$, yielding a simulation covering the fully dealiased range of $5 \leq k_\perp \rho_i \leq 105$, or $0.12 \leq k_\perp \rho_e \leq 2.5$. It is worthwhile noting that it has been demonstrated, via comparisons with PIC simulations, that nonlinear gyrokinetic simulations using **AstroGK** accurately describe the physics of magnetic reconnection in the strong guide field limit, as long as the simulation resolves the electron Larmor radius scale (TenBarge *et al.* 2014).

The simulation is driven at the domain scale using an oscillating Langevin antenna (TenBarge *et al.* 2014) to achieve turbulence with a nonlinearity parameter $\chi \sim 1$, yielding critically balanced, strong turbulent cascade of kinetic Alfvén waves (Goldreich & Sridhar 1995; Howes *et al.* 2008*a*, 2011; TenBarge *et al.* 2014). The linear frequency of a kinetic Alfvén wave at the domain scale, determined by the collisionless linear gyrokinetic dispersion relation (Howes *et al.* 2006), is given by $\omega = 3.6\omega_{A0}$, where $\omega_{A0} = k_{\parallel 0}v_A$. The parameters of the oscillating Langevin antenna are amplitude $A_0 = 0.2$, driving frequency $\omega_0 = 3.6\omega_{A0}$, and decorrelation rate $\gamma_0 = 0.6\omega_{A0}$. We drive four modes, $(k_{\perp 0}\rho_i, k_{\perp 0}\rho_i, k_{\parallel 0}\rho_i/\epsilon) = (5, 0, \pm 1)$ and $(0, 5, \pm 1)$, where $k_{\perp 0} = 2\pi/L_\perp$ and $k_{\parallel 0} = 2\pi/L_z$. Note that the 3D simulation spatial domain has size $L_\perp^2 \times L_z$, with $L_\perp = 2\pi\rho_i/5$ and $L_z = 2\pi\rho_i/(5\epsilon)$, where $\epsilon \ll 1$ is the arbitrary gyrokinetic expansion parameter. These parameters are found to yield a statistically steady-state value of the nonlinearity parameter of $\chi \simeq 1$.

Collision frequencies $\nu_i = 0.2\omega_{A0}$ and $\nu_e = 0.5\omega_{A0}$ are chosen to prevent a build-up of small-scale structure in velocity space, yet to avoid altering the weakly collisional dynamics, $\nu_s \ll \omega$. All dissipation required to achieve a statistically steady state in the simulation occurs via physically resolved interactions, primarily collisionless damping via the Landau resonance with electrons; no additional hypercollisionality is needed in this simulation.

5. Development and Saturation of Turbulent Cascade and Magnetic Field Line Wander

In this section, we present numerical results describing the development and saturation of the turbulent magnetic energy spectrum and of the magnetic field line wander. In addition, we use Poincare plots to characterize the development of stochasticity in the magnetic field.

5.1. Development and Saturation of Turbulent Magnetic Energy Spectrum

These driven turbulence simulations begin with a straight, uniform magnetic field and zero fluctuations. The oscillating Langevin antenna drives an external parallel current that generates perpendicular magnetic field fluctuations, each driven mode with a plane-wave pattern specified by the wavevector. Nonlinear interactions between the counter-propagating Alfvén waves generated by the antenna immediately begin to transfer energy to higher wavenumbers, and the magnetic energy spectrum begins to fill in as energy is continually injected into the driven modes. Figure 6 presents the perpendicular magnetic energy spectrum $E_{B_\perp}(k_\perp) = \int_{-\infty}^{\infty} dk_z \int_0^{2\pi} d\theta k_\perp |\delta B(k_\perp)|^2 / 8\pi$ at a number of times early

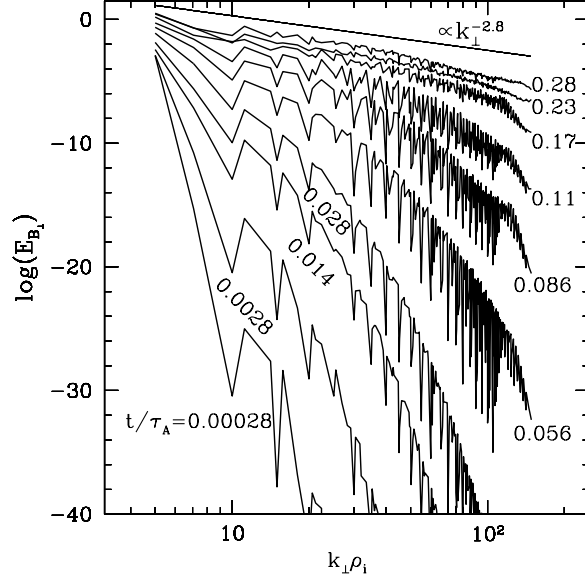


FIGURE 6. Development of the magnetic energy spectrum in the nonlinear gyrokinetic simulation of driven kinetic Alfvén wave turbulence. The normalized time for each spectrum t/τ_A is labeled. The saturated spectrum for strong kinetic-Alfvén -wave cascade is expected to have a spectral index of -2.8 , plotted for comparison.

in the development of the turbulent energy spectrum, where time is normalized using the linear kinetic Alfvén wave period for modes at the domain scale, t/τ_A and $\omega_{A0}\tau_A = 1.74$. Note that, due to the broad range of the logarithmic vertical axis, at the very early times $t/\tau_A < 0.1$, very little energy has been injected into the turbulent cascade.

Figure 7 shows how the spectrum saturates to a statistically steady state. Ten perpendicular magnetic energy spectra (blue and black) are plotted at uniform linear time intervals $t_j/\tau_A = j\Delta t/\tau_A$ for $j = 1, 2, 3, \dots, 10$ and $\Delta t/\tau_A = 0.028$. We also overplot all spectra over the time range $0.28 \leq t/\tau_A \leq 3.6$ (red). This plot shows that, although, more energy is injected into the turbulent magnetic energy spectrum at $t/\tau_A > 0.28$, the shape of the spectrum appears to be saturated at $t/\tau_A = 0.28$ —only the total energy content changes, but the shape of the spectrum does not. We also plot the exponentially cutoff magnetic energy spectrum (blue dashed) determined empirically from a sample of 100 *Cluster* spectra, $E_{B\perp}(k_{\perp}) \propto (k_{\perp}\rho_i)^{-2.8} \exp(-k_{\perp}\rho_e)$ (Alexandrova *et al.* 2012), a result reproduced previously using nonlinear gyrokinetic simulations (TenBarge & Howes 2013; TenBarge *et al.* 2013). The present simulation also agrees well with this model magnetic energy spectrum.

Note that the spectra in Figure 7 have been binned in bins of width $\Delta k_{\perp}\rho_i = 5$, producing a smoother appearance than the spectra in Figure 6, in which all possible values of $k_{\perp}\rho_i$ from our perpendicular wavevector grid are represented.

The timescales associated with the development and saturation of the turbulent cascade can be nicely illustrated by plotting the amplitude of the energy at a perpendicular wavenumber in the middle of the dynamic range at $k_{\perp}\rho_i = 20.6$ as a function of time, as shown in Figure 8(a). At early times $t/\tau_A < 0.14$, the perpendicular magnetic energy at $k_{\perp}\rho_i = 20.6$ increases as a steep power law with time, $E_{B\perp}(k_{\perp}) \propto t^{12}$. At time $t_1/\tau_A = 0.14$, the increase of energy with time at this wavenumber reduces to a less

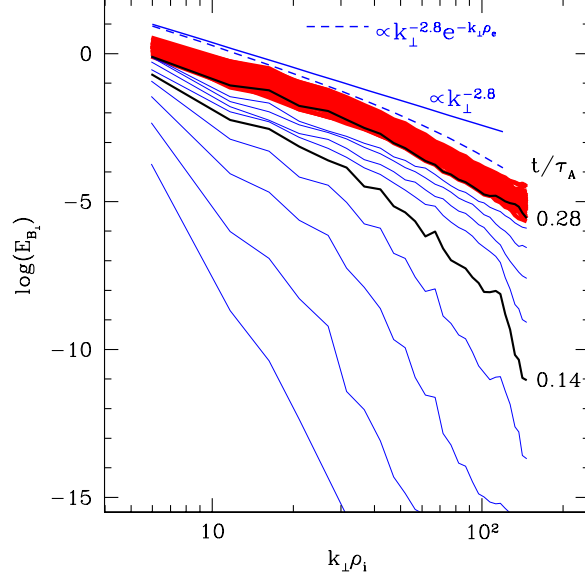


FIGURE 7. Perpendicular magnetic energy spectra plotted at uniform time intervals of $\delta t/\tau_A = 0.028$ (blue and black), and all spectra overplotted over the range $0.28 \leq t/\tau_A \leq 3.6$ (red). For comparison, the slope for a power-law spectrum $E_{B\perp} \propto k_{\perp}^{-2.8}$ (blue solid) and an exponentially cutoff spectrum $E_{B\perp} \propto k_{\perp}^{-2.8} e^{-k_{\perp}\rho_i}$ (blue dashed) are shown for comparison.

steep approximate power law with $E_{B\perp}(k_{\perp}) \propto k_{\perp}^6$, before reaching a statistically steady value at $t_2/\tau_A = 0.28$.[†] Beyond this time, the shape of the magnetic energy spectrum no longer evolves, as illustrated by the spectra plotted in Figure 7, but the total amplitude of the energy varies over a factor of four, with the same spectral shape simply shifting up and down. This variation of the total energy in the spectrum is due to the fact that the finite-time-correlated driving of the oscillating Langevin antenna leads to a significant variation in the rate of energy injection (TenBarge *et al.* 2014).

It is worthwhile pointing out how rapidly the magnetic energy spectrum saturates, requiring a length of time that is only a fraction of the period of the kinetic Alfvén wave at the domain scale, $0.28\tau_A$. This is likely due to the dispersive nature of the kinetic Alfvén wave fluctuations in the sub-ion length scale regime. $k_{\perp}\rho_i \gg 1$, where the parallel phase velocity of the waves increases linearly with $k_{\perp}\rho_i$, with an approximate scaling (Howes *et al.* 2014)

$$\frac{\omega}{k_{\parallel}} = v_A \frac{k_{\perp}\rho_i}{\sqrt{\beta_i + 2/(1 + T_e/T_i)}}. \quad (5.1)$$

Thus, the increasingly fast dynamics of the fluctuations with decreasing scale appears to saturate the energy spectrum more rapidly than the wave period of the domain scale kinetic Alfvén waves that drive the cascade. It is also worthwhile noting that the turbulent cascade is very efficiently generated by driving counterpropagating kinetic Alfvén waves at the domain scale.

In Figure 8(b), we plot the evolution of the spectral index η of the perpendicular

[†] Note that the power law scaling of the amplitude reported here is dependent on the value of $k_{\perp}\rho_i$ chosen. A detailed study of how this scaling varies with $k_{\perp}\rho_i$ is beyond the scope of the work presented here.

magnetic spectrum E_{B_\perp} as a function of normalized time t/τ_A . To determine the value of the spectral index, we perform a fit of the perpendicular magnetic spectrum at each time using the form

$$E_{B_\perp} \propto (k_\perp \rho_i)^\eta \exp[-k_\perp \rho_e] \quad (5.2)$$

over the range of scales $10 \leq k_\perp \rho_i \leq 105$. As shown in panel (b), the rate of increase of the spectral index decreases, particularly for $t > t_1$, finally saturating to a constant value for $t \geq t_2$.

5.2. Development and Saturation of Magnetic Field Line Wander

To estimate the development and saturation of magnetic field line wander, we devise a new diagnostic, the *expansion parameter* σ , derived in Appendix A. This diagnostic yields a scalar quantity that parameterizes the separation of magnetic field lines in the turbulent magnetic field throughout the simulation domain.

In Figure 8(c), we plot the evolution of expansion parameter σ as a function of normalized time t/τ_A . We plot the results for two independent simulations (red and blue), with all of the same numerical and physical parameters, but different pseudo-random number sequences governing the driving by the oscillating Langevin antenna. The expansion parameter σ increases as a power law right up to the time $t_2/\tau_A = 0.28$, at which point σ saturates to a statistically steady value. Note that unlike in panel (a), where the rate of increase of amplitude of turbulent cascade shows a marked decrease at time $t = t_1$, the power-law increase of the expansion parameter σ in panel (c) shows little change at $t = t_1$. Note also that the two independent simulations generate statistically similar results for the evolution of this expansion parameter σ . Therefore, it appears for these simulations with plasma parameters $\beta_i = 1$ and $T_i/T_e = 1$ and turbulent amplitude $\chi \simeq 1$, the magnetic field line separation appears to saturate on the same timescale as the turbulent magnetic energy spectrum.

6. Development of Magnetic Stochasticity

In well developed turbulence, the magnetic field appears to become tangled up in a stochastic manner, raising two very important questions about the development of magnetic stochasticity in turbulent plasmas. First, how long must the turbulence evolve before the magnetic field becomes stochastic? Second, must the amplitude of the turbulence exceed some threshold value for the development of stochasticity? We reiterate here that we reserve the term “stochastic magnetic field” for a field topology that displays a stochastic nature in a Poincare plot (see below), whereas we employ the term “magnetic field line wander” for the general case of a turbulent magnetic field, whether or not that field demonstrates a stochastic character.

Although Figure 8(c) shows the timescale of the saturation of the separation of magnetic field lines, as diagnosed by the scalar expansion parameter σ , it does not provide alone any information about whether the magnetic field has become stochastic. To investigate the development of stochasticity, we use Poincare plots to yield a qualitative measure of the stochasticity (Dombre *et al.* 1986; Wang *et al.* 2011; Nevins *et al.* 2011).

To construct the Poincare plot, we begin with the magnetic field $\mathbf{B}(\mathbf{x})$ at some time t . On the perpendicular plane at one end of the simulation domain at $z = 0$, we specify a sparse pattern of points with the color of each point creating a bullseye pattern. The magnetic field line passing through each point is traced through the domain to the far end of the simulation domain at $z = L_z$, and a point is plotted there, with color matching that of the original field line position. That field line is periodically wrapped to $z = 0$,

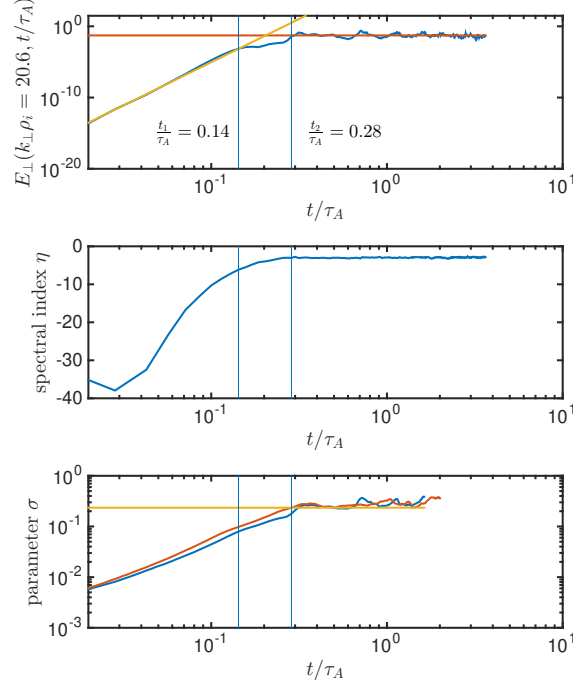


FIGURE 8. (a) Evolution of the energy in modes with $k_\perp \rho_i = 20.6$ vs. normalized time t/τ_A , showing power-law growth until $t_1/\tau_A = 0.14$, and a slower growth until $t_2/\tau_A = 0.28$ (b) Evolution of the spectral index, η , where the spectrum is fit by $(k_\perp \rho_i)^\eta \exp(-k_\perp \rho_e)$, showing saturation at time $t_2/\tau_A = 0.28$. (c) Evolution of the scalar expansion parameter σ , showing that the separation of field lines saturates only at $t_2/\tau_A = 0.28$, with little noticeable change at $t_1/\tau_A = 0.14$. A second identical run (with a different pseudo-random number sequence governing the forcing) shows the evolution is statistically repeatable.

and the process is continued, with a colored point plotted at each crossing at $z = L_z$. We trace through the box 20 times for each field line, generating a sufficient number of points in the Poincare plot to visually determine whether or not the magnetic field has become stochastic. A fourth-order Runge-Kutta method with adaptive step-size is used to trace each field line by integrating the ordinary differential equation $d\mathbf{r}/dl = \hat{\mathbf{b}}(\mathbf{x})$, where $\hat{\mathbf{b}}(\mathbf{x}) = \mathbf{B}(\mathbf{x})/|\mathbf{B}(\mathbf{x})|$. If the field line passes through the boundaries of the simulation domain in the x or y directions, it is periodically wrapped to the opposite boundary. We have checked that using the field-line following routine to trace back down the field line returns to the original starting point.

Figure 9 shows the Poincare plots for the magnetic field at times $t/\tau_A = 0.083, 0.154, 0.226$, and 3.052 . At the early time $t_1/\tau_A = 0.083$, the Poincare plot remains well ordered, indicating that the magnetic field has not yet become stochastic. By the time $t/\tau_A = 0.155$, some regions of the Poincare plot demonstrate a disordered mixture of colored points, indicating regions that have become stochastic, while other regions maintain some semblance of order. Thus, it appears that as the magnetic field becomes stochastic, that stochasticity manifests itself in some regions of the domain but not others. By time $t/\tau_A = 0.226$, the entire domain demonstrates a stochastic character. Since the turbulent spectrum appears to saturate to a constant shape at $t_2/\tau_A = 0.28$, we conclude that,

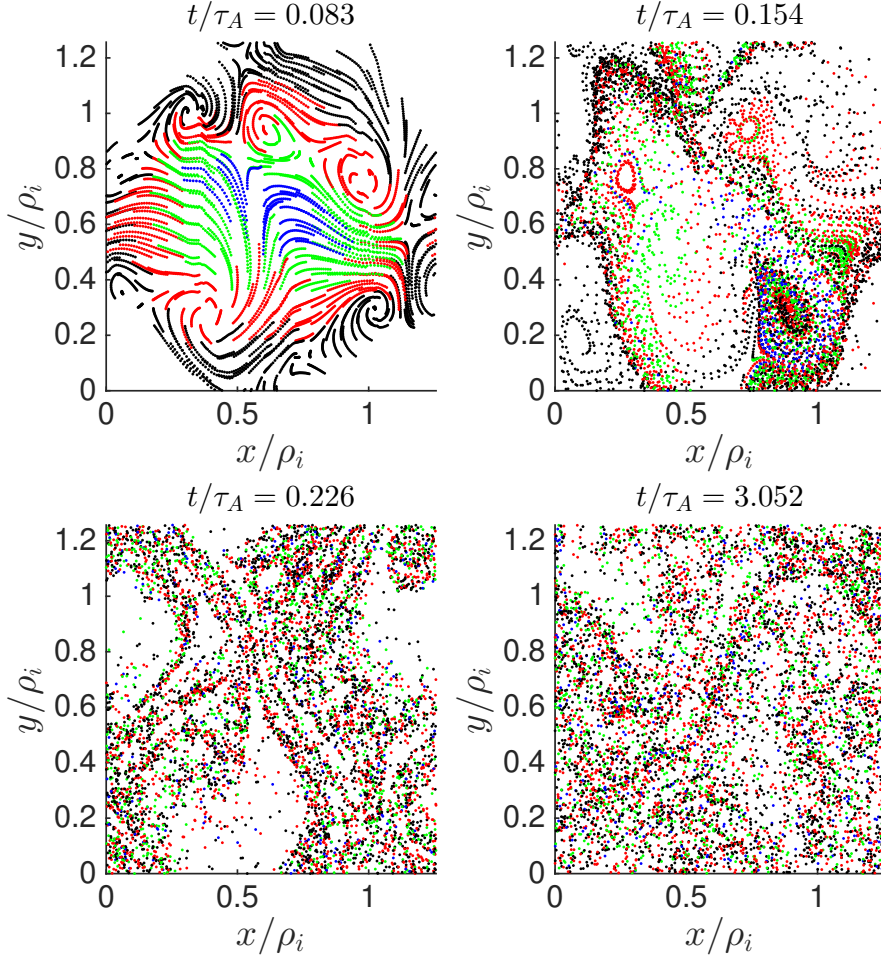


FIGURE 9. Poincaré plots in the $z = L_z$ plane that diagnose the magnetic field topology at times $t/\tau_A = 0.083, 0.154, 0.226$, and 3.052 , showing regions of stochasticity at $t/\tau_A = 0.154$ and fully developed stochasticity for $t/\tau_A \gtrsim 0.226$.

for this critically balanced simulation with nonlinearity parameter $\chi \sim 1$, the magnetic field is generically stochastic for well developed turbulence. Since space and astrophysical plasmas are almost always found to be turbulent, this finding has significant implications for many systems of interest.

Note that we can use these results to relate indirectly the expansion parameter σ to the development of stochasticity of the magnetic field. The expansion parameter has the advantage that it can be computed locally, depending only on the value of the magnetic field and its derivatives at a single point, whereas the computation of the Poincaré plot requires knowledge of the magnetic field throughout the simulation domain. Future work will more thoroughly compare the expansion parameter σ to Poincaré plots for cases of turbulence with different amplitudes to determine whether the σ can be useful as a proxy to estimate the stochasticity of a given magnetic field configuration.

7. Conclusion

Here we have presented a general context for understanding the tangling of magnetic lines in a turbulent plasma from direct numerical simulations of weakly collisional plasma turbulence. We have discussed the broader issue of magnetic field line wander, including the effect on the propagation of cosmic rays and energetic particles in the heliosphere and other astrophysical plasmas, the degradation of particle confinement in magnetic fusion devices, the relation to the cascade of energy in plasma turbulence, and the role played by tangled magnetic fields in particle acceleration and magnetic reconnection. We have identified some key questions about the development and saturation of magnetic field line wander in plasma turbulence, and discussed the fundamental turbulence and plasma parameters upon which this behavior is likely to depend.

We present the analysis of a driven kinetic Alfvén wave simulation of strong plasma turbulence with plasma parameters $\beta_i = 1$ and $T_i/T_e = 1$ and a nonlinearity parameter $\chi \simeq 1$. We show how the magnetic energy spectrum develops in time from uniform conditions and saturates to a steady spectral shape, and identify two timescales that characterize the evolution and saturation. Next, we investigate the development of tangling in the magnetic field using a scalar expansion parameter σ to characterize the separation of field lines in the plasma turbulence. Finally, we use Poincare plots to qualitatively demonstrate how the magnetic field attains a stochastic character in our strong plasma turbulence simulation.

We find that, for the case of strong plasma turbulence analyzed here, the magnetic field indeed develops a stochastic character. We expect that, on general grounds, the magnetic field in turbulent space and astrophysical plasmas is likely to always be stochastic. Such a stochastic nature of the magnetic field is very important to the prediction of the propagation of energetic particles through the turbulence heliospheric interplanetary magnetic field, with implications for energetic particles hazards to spaceborne robotic and human assets.

The companion work to this paper, ?, explores the magnetic field line wander over a range of turbulent amplitudes $0.1 \lesssim \chi \lesssim 5$ with $\beta_i = 1$ and $T_i/T_e = 1$ to test whether one should indeed always expect turbulent astrophysical plasmas to contain a stochastic magnetic field. We find that the magnetic field becomes fully stochastic when the turbulence amplitude exceeds a threshold value, $\chi > \chi_{\text{thresh}} \simeq 0.1$. Analysis of the spreading of the field lines finds slightly superdiffusive behavior for stronger turbulence with $\chi > 1$ and slightly subdiffusive behavior for weaker turbulence with $\chi < 1$, and we provide a functional form for the dependence on the turbulent amplitude χ for the coefficient $A(\chi)$ and exponent $p(\chi)$ in (3.1). For the case of critically balanced turbulence with $\chi \sim 1$, the behavior appears to be quite close to diffusive, with the exponent in (3.1) given by $p(\chi = 1) \simeq 1$. This appears to be in agreement with the Rechester-Rosenbluth model of diffusive behavior (Rechester & Rosenbluth 1978), although away from critical balance the direct numerical simulations suggest this simple model may break down.

Appendix A. Definition of the Scalar Expansion Parameter σ

It is useful to derive a scalar quantity that can parameterize the separation of field lines in a turbulent magnetic field. For this purpose, we derive here the scalar *expansion parameter*, σ .

We begin with the magnetic field specified throughout the triply periodic simulation domain at a single time, $\mathbf{B}(\mathbf{x})$. We define the unit vector that specifies local direction of

the magnetic field,

$$\hat{\mathbf{b}}(\mathbf{x}) \equiv \frac{\mathbf{B}(\mathbf{x})}{|\mathbf{B}(\mathbf{x})|}, \quad (\text{A } 1)$$

where $\mathbf{x} = (x, y, z)$ is the position. Field-line tracing can be performed by following along the local magnetic field direction at each point,

$$\frac{\partial \mathbf{r}}{\partial l} = \hat{\mathbf{b}}(\mathbf{r}), \quad (\text{A } 2)$$

where l is the distance along the magnetic field line. A field line is defined by the vector $\mathbf{r}(l, \mathbf{r}_0)$, where the starting point at $l = 0$ is $\mathbf{r}_0 = \mathbf{r}(0, \mathbf{r}_0)$.

Since we are interested in the separation between field lines as you progress along either of those field lines, we chose another field line \mathbf{r}' separated from the field line \mathbf{r} by the separation $\delta \mathbf{r}$, such that $\mathbf{r}'(l, \mathbf{r}'_0) = \mathbf{r}(l, \mathbf{r}_0) + \delta \mathbf{r}(l)$. Taylor expanding the field line \mathbf{r}' about \mathbf{r} , one may obtain an expression for the evolution of $\delta \mathbf{r}$ as you move a distance l along the field line \mathbf{r} ,

$$\frac{\partial \delta \mathbf{r}}{\partial l} = (\delta \mathbf{r} \cdot \nabla) \hat{\mathbf{b}}(\mathbf{r}) \quad (\text{A } 3)$$

Since we are primarily interested here in the separation of magnetic field lines due to turbulence at scales sufficiently below the outer scale of the inertial range, we take the local magnetic field to be $\mathbf{B}(\mathbf{x}) = B_0 \hat{\mathbf{z}} + \delta \mathbf{B}(\mathbf{x})$, where the perturbations are small compared to the mean magnetic field, $|\delta \mathbf{B}| \ll B_0$. In this limit, the total magnetic field magnitude

$$B = |\mathbf{B}| = \sqrt{B_0^2 + 2B_0\delta B_z + |\delta \mathbf{B}|^2} \simeq B_0 + \delta B_z + \mathcal{O}(|\delta \mathbf{B}|^2) \quad (\text{A } 4)$$

Substituting this result into the definition of $\hat{\mathbf{b}}$ and dropping terms of order $\mathcal{O}(|\delta \mathbf{B}|^2/B_0^2)$ and higher, we obtain a first-order expression for the magnetic field direction,

$$\hat{\mathbf{b}}(\mathbf{r}) = \hat{\mathbf{z}} + b_x \hat{\mathbf{x}} + b_y \hat{\mathbf{y}}, \quad (\text{A } 5)$$

where $b_x = \delta B_x/B_0$ and $b_y = \delta B_y/B_0$. Therefore, to first order, the variation of the direction of the magnetic field depends only on the components of the magnetic field perpendicular to the mean magnetic field, $\mathbf{B}_0 = B_0 \hat{\mathbf{z}}$. In this limit, to first order in $|\delta \mathbf{B}|$, we may express the displacement of the magnetic field lines $\delta \mathbf{r}(l)$ in terms of the initial displacement $\delta \mathbf{r}_0$ by

$$\delta \mathbf{r}(l) = \alpha(l) R[\phi(l)] \cdot \delta \mathbf{r}_0, \quad (\text{A } 6)$$

where $\alpha(l)$ represents expansion (positive) or contraction (negative) of the separation between the field lines, and $R[\phi(l)]$ is a matrix representing rotation *in the perpendicular plane* of the vector by an angle $\phi(l)$,

$$R[\phi(l)] \equiv \begin{pmatrix} \cos[\phi(l)] & -\sin[\phi(l)] \\ \sin[\phi(l)] & \cos[\phi(l)] \end{pmatrix}. \quad (\text{A } 7)$$

Thus, the evolution of the displacement (in the perpendicular plane, to lowest order) between two particular magnetic field lines may be characterized by the two scalar quantities $\alpha(l)$ and $\phi(l)$.

Here we are primarily interested in the separation of field lines $\alpha(l)$, so we eliminate $\phi(l)$ by taking a dot product of (A 6) with itself, obtaining the result,

$$|\delta \mathbf{r}|^2 = \alpha^2 |\delta \mathbf{r}_0|^2 \quad (\text{A } 8)$$

We can obtain an expression for α by using (A 3) to obtain

$$\delta \mathbf{r} = \delta l (\delta \mathbf{r}_0 \cdot \nabla) \hat{\mathbf{b}}(\mathbf{r}_0) + \delta \mathbf{r}_0, \quad (\text{A } 9)$$

an expression for the separation valid to first order in δl . One may then obtain the expression, valid to first order in δl ,

$$\alpha = \frac{|\delta \mathbf{r}|}{|\delta \mathbf{r}_0|} = 1 + \frac{\delta \mathbf{r}_0 \cdot [(\delta \mathbf{r}_0 \cdot \nabla) \hat{\mathbf{b}}(\mathbf{r}_0)]}{|\delta \mathbf{r}_0|^2} \delta l. \quad (\text{A } 10)$$

Finally, we define the dimensionless scalar *expansion parameter*, σ , by

$$\frac{\partial(\delta r/\rho_i)}{\partial(l/a_0)} = \sigma(\delta r_0/\rho_i) \quad (\text{A } 11)$$

where the perpendicular length scale is normalized by the ion thermal Larmor radius $\rho_i = v_{ti}/\Omega_i = (2T_i/m_i)^{1/2} m_i c/q_i B_0$ and the parallel length scale is normalized by a characteristic length a_0 . Note that by normalizing to two separate length scales, this definition enables a strong connection to gyrokinetic simulations in which the gyrokinetic expansion parameter, $\epsilon \equiv \rho_i/a_0 \sim |\delta \mathbf{B}|/B_0 \ll 1$, enables the results of a single simulation to be scaled to any ratio for the strength of the equilibrium field to the perturbed magnetic field, $B_0/|\delta \mathbf{B}| \sim a_0/\rho_i$. This expression can be simplified to

$$\frac{\partial \delta r}{\partial l} = \sigma \left(\frac{\delta r_0}{\rho_i} \right) \left(\frac{\rho_i}{a_0} \right), \quad (\text{A } 12)$$

where the presence of the gyrokinetic expansion parameter in the last pair of parentheses yields a value of σ of similar magnitude for different ratios of $B_0/|\delta \mathbf{B}|$.

In the limit $\delta l \rightarrow 0$, this dictates $\delta r = \delta r_0 + (\sigma \delta l/a_0) \delta r_0$. Comparing this expression for α in (A 10), and using (A 8), we obtain a simple result for the expansion parameter,

$$\sigma = \delta \hat{\mathbf{r}}_0 \cdot [(\delta \hat{\mathbf{r}}_0 \cdot \hat{\nabla}) \hat{\mathbf{b}}(\mathbf{r}_0)], \quad (\text{A } 13)$$

where we define the direction of the initial separation vector $\delta \hat{\mathbf{r}}_0 = \delta \mathbf{r}_0/\delta r_0$. In addition, we have normalized the gradient operator to the ion Larmor radius scale, so that the perpendicular components of this operator (the only ones that contribute to (A 13)) are given by $\hat{\nabla}_\perp = \hat{\mathbf{x}}\rho_i(\partial/\partial x) + \hat{\mathbf{y}}\rho_i(\partial/\partial y)$. If we take an initial separation vector to have an angle γ in the x - y plane with respect to the x -axis, $\delta \hat{\mathbf{r}}_0 = \cos \gamma \hat{\mathbf{x}} + \sin \gamma \hat{\mathbf{y}}$, then this expression simplifies to

$$\sigma = \cos^2 \gamma \frac{\partial b_x}{\partial x} + \sin \gamma \cos \gamma \left(\frac{\partial b_y}{\partial x} + \frac{\partial b_x}{\partial y} \right) + \sin^2 \gamma \frac{\partial b_y}{\partial y} \quad (\text{A } 14)$$

In the limit $|\delta \mathbf{B}| \ll B_0$, one may obtain an expression for $\hat{\mathbf{b}}$ up to $\mathcal{O}(|\delta \mathbf{B}|^2/B_0^2)$,

$$\hat{\mathbf{b}} = \frac{\mathbf{B}}{|\mathbf{B}|} = \hat{\mathbf{z}} \left(1 + \frac{|\delta \mathbf{B}|^2}{B_0^2} \right) + \frac{\delta B_x}{B_0} \hat{\mathbf{x}} + \frac{\delta B_y}{B_0} \hat{\mathbf{y}} - \frac{\delta B_z}{B_0} \frac{\delta \mathbf{B}}{B_0}. \quad (\text{A } 15)$$

Taking the divergence of the field direction, we obtain

$$\nabla \cdot \hat{\mathbf{b}} = \frac{\partial}{\partial x} \left(\frac{\delta B_x}{B_0} \right) + \frac{\partial}{\partial y} \left(\frac{\delta B_y}{B_0} \right) - \frac{\partial}{\partial x} \left(\frac{\delta B_x \delta B_z}{B_0^2} \right) - \frac{\partial}{\partial y} \left(\frac{\delta B_y \delta B_z}{B_0^2} \right) - \frac{\partial}{\partial z} \left(\frac{\delta B_x^2 \delta B_y^2}{B_0^2} \right) \quad (\text{A } 16)$$

In the anisotropic limit $\epsilon \equiv k_\parallel/k_\perp \sim |\delta \mathbf{B}|/B_0 \ll 1$ that is relevant to turbulent fluctuations at small scales, then $\partial/\partial z \sim \epsilon \partial/\partial x \sim \epsilon \partial/\partial y$, and the terms in the equations above have the following order: the first two terms are $\mathcal{O}(\epsilon)$, the next two terms are $\mathcal{O}(\epsilon^2)$, and

the final term is $\mathcal{O}(\epsilon^3)$. Therefore, dropping terms of order $\mathcal{O}(\epsilon^2)$ and higher, we obtain the simplified expression,

$$\nabla \cdot \hat{\mathbf{b}}_{\perp} = 0, \quad (\text{A } 17)$$

where $\hat{\mathbf{b}}_{\perp} = \delta B_x/B_0 \hat{\mathbf{x}} + \delta B_y/B_0 \hat{\mathbf{y}}$. Therefore, we obtain the important simplifying result, $\partial b_x/\partial x = -\partial b_y/\partial y$. This important result means that, to lowest order, compressions and expansions of the magnetic field are divergence free in the perpendicular plane.

One consequence of this property is that, for a given initial field line, \mathbf{r} , the expansion parameter σ yields a zero value when integrated over all possible directions γ of displacement about that point. Specifically,

$$\int_0^{2\pi} d\gamma \sigma(\gamma) = \int_0^{2\pi} d\gamma \left[\cos^2 \gamma \frac{\partial b_x}{\partial x} + \sin \gamma \cos \gamma \left(\frac{\partial b_y}{\partial x} + \frac{\partial b_x}{\partial y} \right) + \sin^2 \gamma \frac{\partial b_y}{\partial y} \right] \quad (\text{A } 18)$$

$$= \frac{1}{2} \left(\frac{\partial b_x}{\partial x} + \frac{\partial b_y}{\partial y} \right) = 0 \quad (\text{A } 19)$$

Note that the values of the derivatives $\partial b_i/\partial x_j$ are constant in this integration.

The consequence of this finding is that the value of the expansion parameter as a function of angle γ is bounded by some maximum value, $|\sigma(\gamma)| \leq \sigma_{max}$. Thus, at each point \mathbf{r} , we can simply use this maximum value as a scalar value that simply characterizes the expansion (and the consequent equal and opposite contraction at other angles necessary to yield $\int_0^{2\pi} d\gamma \sigma(\gamma) = 0$). In the body of the paper, the parameter σ at a given instant of time is computed as the value of σ_{max} averaged over all points in the simulation domain.

A treatment of the twisting of the magnetic field about itself, characterized by the parameter $\phi(l)$, will be presented in subsequent work.

The work has been supported by NSF CAREER Award AGS-1054061 and NASA NNX10AC91G.

REFERENCES

- ABEL, I. G., BARNES, M., COWLEY, S. C., DORLAND, W. & SCHEKOCHIHIN, A. A. 2008 Linearized model Fokker-Planck collision operators for gyrokinetic simulations. I. Theory. *Phys. Plasmas* **15** (12), 122509.
- ALEXandrova, O., LACOMBE, C., MANGENEY, A., GRAPPIN, R. & MAKsimovic, M. 2012 Solar Wind Turbulent Spectrum at Plasma Kinetic Scales. *Astrophys. J.* **760**, 121.
- ALEXandrova, O., SAUR, J., LACOMBE, C., MANGENEY, A., MITCHELL, J., SCHWARTZ, S. J. & ROBERT, P. 2009 Universality of Solar-Wind Turbulent Spectrum from MHD to Electron Scales. *Phys. Rev. Lett.* **103** (16), 165003.
- BARNES, M., ABEL, I. G., DORLAND, W., ERNST, D. R., HAMMETT, G. W., RICCI, P., ROGERS, B. N., SCHEKOCHIHIN, A. A. & TATSUNO, T. 2009 Linearized model Fokker-Planck collision operators for gyrokinetic simulations. II. Numerical implementation and tests. *Phys. Plasmas* **16** (7), 072107.
- BELCHER, J. W. & DAVIS, L. 1971 Large-Amplitude Alfvén Waves in the Interplanetary Medium, 2. *J. Geophys. Res.* **76**, 3534–3563.
- BIAN, N. H., KONTAR, E. P. & MACKINNON, A. L. 2011 Turbulent cross-field transport of non-thermal electrons in coronal loops: theory and observations. *Astron. Astrophys.* **535**, A18.
- BIEBER, J. W., WANNER, W. & MATTHAEUS, W. H. 1996 Dominant two-dimensional solar wind turbulence with implications for cosmic ray transport. *J. Geophys. Res.* **101**, 2511–2522.
- BOOZER, A. H. 2014 Formation of current sheets in magnetic reconnection. *Phys. Plasmas* **21** (7), 072907.
- BOUROUAINE, S., ALEXandrova, O., MARSCH, E. & MAKsimovic, M. 2012 On Spectral

- Breaks in the Power Spectra of Magnetic Fluctuations in Fast Solar Wind between 0.3 and 0.9 AU. *Astrophys. J.* **749**, 102.
- BRUNO, R. & CARBONE, V. 2005 The Solar Wind as a Turbulence Laboratory. *Living Reviews in Solar Physics* **2**, 4.
- CHANDRAN, B. D. G. 2000 Scattering of Energetic Particles by Anisotropic Magnetohydrodynamic Turbulence with a Goldreich-Sridhar Power Spectrum. *Phys. Rev. Lett.* **85**, 4656–4659.
- CHANDRAN, B. D. G. & COWLEY, S. C. 1998 Thermal Conduction in a Tangled Magnetic Field. *Phys. Rev. Lett.* **80**, 3077–3080.
- CHANDRASEKHAR, S. 1951 The Invariant Theory of Isotropic Turbulence in Magneto-Hydrodynamics. *Proceedings of the Royal Society of London Series A* **204**, 435–449.
- CHEN, C. H. K., HORBURY, T. S., SCHEKOCHIHIN, A. A., WICKS, R. T., ALEXANDROVA, O. & MITCHELL, J. 2010 Anisotropy of Solar Wind Turbulence between Ion and Electron Scales. *Phys. Rev. Lett.* **104** (25), 255002.
- CHO, J. & LAZARIAN, A. 2004 The Anisotropy of Electron Magnetohydrodynamic Turbulence. *Astrophys. J. Lett.* **615**, L41–L44.
- CHO, J. & LAZARIAN, A. 2009 Simulations of Electron Magnetohydrodynamic Turbulence. *Astrophys. J.* **701**, 236–252.
- CHO, J. & VISHNIAC, E. T. 2000 The Anisotropy of Magnetohydrodynamic Alfvénic Turbulence. *Astrophys. J.* **539**, 273–282.
- DEL-CASTILLO-NEGRETTE, D. & BLAZEVSKEI, D. 2014 Heat pulse propagation in chaotic three-dimensional magnetic fields. *Nuclear Fusion* **54** (6), 064009.
- DEL-CASTILLO-NEGRETTE, D. & BLAZEVSKEI, D. 2016 Modulated heat pulse propagation and partial transport barriers in chaotic magnetic fields. *Physics of Plasmas* **23** (4), 042505.
- DOMBRE, T., FRISCH, U., HENON, M., GREENE, J. M. & SOWARD, A. M. 1986 Chaotic streamlines in the ABC flows. *J. Fluid Mech.* **167**, 353–391.
- DRAKE, D. J., SCHROEDER, J. W. R., HOWES, G. G., KLETZING, C. A., SKIFF, F., CARTER, T. A. & AUERBACH, D. W. 2013 Alfvén wave collisions, the fundamental building block of plasma turbulence. IV. Laboratory experiment. *Physics of Plasmas* **20** (7), 072901.
- EYINK, G., VISHNIAC, E., LALESCU, C., ALUIE, H., KANOV, K., BÜRGER, K., BURNS, R., MENEVEAU, C. & SZALAY, A. 2013 Flux-freezing breakdown in high-conductivity magnetohydrodynamic turbulence. *Nature* **497**, 466–469.
- FILONENKO, N. N., SAGDEEV, R. Z. & ZASLAVSKY, G. M. 1967 Destruction of Magnetic Surfaces by Magnetic Field Irregularities. 2. *Nuclear Fusion* **7** (4), 253.
- FRIEMAN, E. A. & CHEN, L. 1982 Nonlinear gyrokinetic equations for low-frequency electromagnetic waves in general plasma equilibria. *Phys. Fluids* **25**, 502–508.
- GALEEV, A. A. & ZELENY, L. M. 1981 Anomalous electron thermal conductivity across the destroyed magnetic surfaces. *Physica D Nonlinear Phenomena* **2**, 90–101.
- GALTIER, S., NAZARENKO, S. V., NEWELL, A. C. & POUQUET, A. 2000 A weak turbulence theory for incompressible magnetohydrodynamics. *J. Plasma Phys.* **63**, 447–488.
- GIACALONE, J. & JOKIPII, J. R. 1999 The Transport of Cosmic Rays across a Turbulent Magnetic Field. *Astrophys. J.* **520**, 204–214.
- GOLDREICH, P. & SRIDHAR, S. 1995 Toward a Theory of Interstellar Turbulence II. Strong Alfvénic Turbulence. *Astrophys. J.* **438**, 763–775.
- GRUZINOV, A. V., ISICHENKO, M. B. & KALDA, I. L. 1990 Two-dimensional turbulent diffusion. *Sov. Phys. JETP* **97**, 476–488.
- GUEST, B. & SHALCHI, A. 2012 Random walk of magnetic field lines in dynamical turbulence: A field line tracing method. II. Two-dimensional turbulence. *Phys. Plasmas* **19** (3), 032902.
- GUO, F. & GIACALONE, J. 2010 The Effect of Large-scale Magnetic Turbulence on the Acceleration of Electrons by Perpendicular Collisionless Shocks. *Astrophys. J.* **715**, 406–411.
- GUO, F. & GIACALONE, J. 2013 The Acceleration of Thermal Protons at Parallel Collisionless Shocks: Three-dimensional Hybrid Simulations. *Astrophys. J.* **773**, 158.
- GUO, F. & GIACALONE, J. 2015 The Acceleration of Electrons at Collisionless Shocks Moving Through a Turbulent Magnetic Field. *Astrophys. J.* **802**, 97.
- HAAS, F. A. & THYAGARAJA, A. 1986 Conceptual and experimental bases of theories of anomalous transport in Tokamaks. *Phys. Rep.* **143**, 241–276.
- HATCH, D. R., PUESCHEL, M. J., JENKO, F., NEVINS, W. M., TERRY, P. W. & DO-

- ERK, H. 2012 Origin of Magnetic Stochasticity and Transport in Plasma Microturbulence. *Phys. Rev. Lett.* **108** (23), 235002.
- HATCH, D. R., PUESCHEL, M. J., JENKO, F., NEVINS, W. M., TERRY, P. W. & DOERK, H. 2013 Magnetic stochasticity and transport due to nonlinearly excited subdominant microtearing modes. *Phys. Plasmas* **20** (1), 012307.
- HAUFF, T., JENKO, F., SHALCHI, A. & SCHLICKEISER, R. 2010 Scaling Theory for Cross-Field Transport of Cosmic Rays in Turbulent Fields. *Astrophys. J.* **711**, 997–1007.
- HOWES, G. G. 2015 A dynamical model of plasma turbulence in the solar wind. *Philosophical Transactions of the Royal Society of London A: Mathematical, Physical and Engineering Sciences* **373** (2041), 20140145.
- HOWES, G. G. 2016 The Dynamical Generation of Current Sheets in Astrophysical Plasma Turbulence. *Astrophys. J. Lett.* **82**, L28.
- HOWES, G. G., COWLEY, S. C., DORLAND, W., HAMMETT, G. W., QUATAERT, E. & SCHEKOCHIHIN, A. A. 2006 Astrophysical Gyrokinetics: Basic Equations and Linear Theory. *Astrophys. J.* **651**, 590–614.
- HOWES, G. G., COWLEY, S. C., DORLAND, W., HAMMETT, G. W., QUATAERT, E. & SCHEKOCHIHIN, A. A. 2008a A model of turbulence in magnetized plasmas: Implications for the dissipation range in the solar wind. *J. Geophys. Res.* **113** (A12), A05103.
- HOWES, G. G., DORLAND, W., COWLEY, S. C., HAMMETT, G. W., QUATAERT, E., SCHEKOCHIHIN, A. A. & TATSUNO, T. 2008b Kinetic Simulations of Magnetized Turbulence in Astrophysical Plasmas. *Phys. Rev. Lett.* **100** (6), 065004.
- HOWES, G. G., DRAKE, D. J., NIELSON, K. D., CARTER, T. A., KLETZING, C. A. & SKIFF, F. 2012 Toward Astrophysical Turbulence in the Laboratory. *Phys. Rev. Lett.* **109** (25), 255001.
- HOWES, G. G., KLEIN, K. G. & TENBARGE, J. M. 2014 Validity of the Taylor Hypothesis for Linear Kinetic Waves in the Weakly Collisional Solar Wind. *Astrophys. J.* **789**, 106.
- HOWES, G. G. & NIELSON, K. D. 2013 Alfvén wave collisions, the fundamental building block of plasma turbulence. I. Asymptotic solution. *Phys. Plasmas* **20** (7), 072302.
- HOWES, G. G., NIELSON, K. D., DRAKE, D. J., SCHROEDER, J. W. R., SKIFF, F., KLETZING, C. A. & CARTER, T. A. 2013 Alfvén wave collisions, the fundamental building block of plasma turbulence. III. Theory for experimental design. *Physics of Plasmas* **20** (7), 072304.
- HOWES, G. G., TENBARGE, J. M. & DORLAND, W. 2011 A weakened cascade model for turbulence in astrophysical plasmas. *Phys. Plasmas* **18**, 102305.
- HOWES, G. G., TENBARGE, J. M., DORLAND, W., QUATAERT, E., SCHEKOCHIHIN, A. A., NUMATA, R. & TATSUNO, T. 2011 Gyrokinetic simulations of solar wind turbulence from ion to electron scales. *Phys. Rev. Lett.* **107**, 035004.
- HUANG, Y.-M., BHATTACHARJEE, A. & BOOZER, A. H. 2014 Rapid Change of Field Line Connectivity and Reconnection in Stochastic Magnetic Fields. *Astrophys. J.* **793**, 106.
- ISICHENKO, M. B. 1992 Percolation, statistical topography, and transport in random media. *Rev. Mod. Phys.* **64**, 961–1043.
- JOKIPII, J. R. 1966 Cosmic-Ray Propagation. I. Charged Particles in a Random Magnetic Field. *Astrophys. J.* **146**, 480.
- JOKIPII, J. R. & PARKER, E. N. 1968 Random Walk of Magnetic Lines of Force in Astrophysics. *Phys. Rev. Lett.* **21**, 44–47.
- KIYANI, K. H., CHAPMAN, S. C., KHOTYANTSEV, Y. V., DUNLOP, M. W. & SAHRAOUI, F. 2009 Global scale-invariant dissipation in collisionless plasma turbulence. *Phys. Rev. Lett.* **103**, 075006.
- KIYANI, K. H., OSMAN, K. T. & CHAPMAN, S. C. 2015 Introduction: Dissipation and heating in solar wind turbulence: from the macro to the micro and back again. *Philosophical Transactions of the Royal Society of London Series A* **373**, 40155.
- KLEIN, K. G., HOWES, G. G. & TENBARGE, J. M. 2014 The Violation of the Taylor Hypothesis in Measurements of Solar Wind Turbulence. *Astrophys. J. Lett.* **790**, L20.
- KOLMOGOROV, A. N. 1941 Dissipation of Energy in Locally Isotropic Turbulence. *Dokl. Akad. Nauk SSSR* **32**, 16.
- KOWAL, G., LAZARIAN, A., VISHNIAC, E. T. & OTMIANOWSKA-MAZUR, K. 2009 Numerical Tests of Fast Reconnection in Weakly Stochastic Magnetic Fields. *Astrophys. J.* **700**, 63–85.

- KOWAL, G., LAZARIAN, A., VISHNIAC, E. T. & OTMIANOWSKA-MAZUR, K. 2012 Reconnection studies under different types of turbulence driving. *Nonlin. Proc. Geophys.* **19**, 297–314.
- KRAICHNAN, R. H. 1965 Inertial range spectrum of hydromagnetic turbulence. *Phys. Fluids* **8**, 1385–1387.
- KROMMES, J. A., OBERMAN, C. & KLEVA, R. G. 1983 Plasma transport in stochastic magnetic fields. Part 3. Kinetics of test particle diffusion. *J. Plasma Phys.* **30**, 11–56.
- LAVAL, G. 1993 Particle diffusion in stochastic magnetic fields. *Phys. Fluids B* **5**, 711–721.
- LAZARIAN, A. & VISHNIAC, E. T. 1999 Reconnection in a Weakly Stochastic Field. *Astrophys. J.* **517**, 700–718.
- MARON, J. & GOLDREICH, P. 2001 Simulations of incompressible magnetohydrodynamic turbulence. *Astrophys. J.* **554**, 1175–1196.
- MATTHAEUS, W. H., GRAY, P. C., PONTIUS, JR., D. H. & BIEBER, J. W. 1995 Spatial Structure and Field-Line Diffusion in Transverse Magnetic Turbulence. *Physical Review Letters* **75**, 2136–2139.
- MATTHAEUS, W. H., OUGHTON, S., PONTIUS, JR., D. H. & ZHOU, Y. 1994 Evolution of energy-containing turbulent eddies in the solar wind. *J. Geophys. Res.* **99**, 19267.
- MONTGOMERY, D. & MATTHAEUS, W. H. 1995 Anisotropic Modal Energy Transfer in Interstellar Turbulence. *Astrophys. J.* **447**, 706.
- MONTGOMERY, D. & TURNER, L. 1981 Anisotropic magnetohydrodynamic turbulence in a strong external magnetic field. *Phys. Fluids* **24**, 825–831.
- NARITA, Y., GARY, S. P., SAITO, S., GLASSMEIER, K.-H. & MOTSCHMANN, U. 2011 Dispersion relation analysis of solar wind turbulence. *Geophys. Res. Lett.* **38**, L05101.
- NEVINS, W. M., WANG, E. & CANDY, J. 2011 Magnetic Stochasticity in Gyrokinetic Simulations of Plasma Microturbulence. *Phys. Rev. Lett.* **106** (6), 065003.
- NG, C. S. & BHATTACHARJEE, A. 1996 Interaction of Shear-Alfvén Wave Packets: Implication for Weak Magnetohydrodynamic Turbulence in Astrophysical Plasmas. *Astrophys. J.* **465**, 845.
- NIELSON, K. D., HOWES, G. G. & DORLAND, W. 2013 Alfvén wave collisions, the fundamental building block of plasma turbulence. II. Numerical solution. *Physics of Plasmas* **20** (7), 072303.
- NUMATA, R., HOWES, G. G., TATSUNO, T., BARNES, M. & DORLAND, W. 2010 AstroGK: Astrophysical gyrokinetics code. *J. Comp. Phys.* **229**, 9347.
- POLITANO, H. & POUQUET, A. 1998 von Kármán-Howarth equation for magnetohydrodynamics and its consequences on third-order longitudinal structure and correlation functions. *Phys. Rev. E* **57**, 21.
- PUESCHEL, M. J., KAMMERER, M. & JENKO, F. 2008 Gyrokinetic turbulence simulations at high plasma beta. *Phys. Plasmas* **15** (10), 102310.
- QIN, G. & SHALCHI, A. 2013 The role of the Kubo number in two-component turbulence. *Phys. Plasmas* **20** (9), 092302.
- RAGOT, B. R. 2001 Magnetic Field Line Wandering and Shock-Front Acceleration: Application to the Radio Emission of SN 1987A. *Astrophys. J.* **547**, 1010–1023.
- RAGOT, B. R. 2011 Statistics of Field-line Dispersal: Random-walk Characterization and Supradiffusive Regime. *Astrophys. J.* **728**, 50.
- RAPPAZZO, A. F. & PARKER, E. N. 2013 Current Sheets Formation in Tangled Coronal Magnetic Fields. *Astrophys. J. Lett.* **773**, L2.
- RECHESTER, A. B. & ROSENBLUTH, M. N. 1978 Electron heat transport in a Tokamak with destroyed magnetic surfaces. *Phys. Rev. Lett.* **40**, 38–41.
- RICHARDSON, I. G., VON ROSENVEINGE, T. T., CANE, H. V., CHRISTIAN, E. R., COHEN, C. M. S., LABRADOR, A. W., LESKE, R. A., MEWALDT, R. A., WIEDENBECK, M. E. & STONE, E. C. 2014 > 25 MeV Proton Events Observed by the High Energy Telescopes on the STEREO A and B Spacecraft and/or at Earth During the First Seven Years of the STEREO Mission. *Sol. Phys.* **289**, 3059–3107.
- ROBERTS, O. W., LI, X. & JESKA, L. 2015 A Statistical Study of the Solar Wind Turbulence at Ion Kinetic Scales Using the k-filtering Technique and Cluster Data. *Astrophys. J.* **802**, 2.
- ROBERTS, O. W., LI, X. & LI, B. 2013 Kinetic Plasma Turbulence in the Fast Solar Wind Measured by Cluster. *Astrophys. J.* **769**, 58.

- ROBINSON, D. C. & RUSBRIDGE, M. G. 1971 Structure of turbulence in the zeta plasma. *Phys. Fluids* **14**, 2499–2511.
- ROSENBLUTH, M. N., SAGDEEV, R. Z., TAYLOR, J. B. & ZASLAVSKY, G. M. 1966 Destruction of magnetic surfaces by magnetic field irregularities. *Nuclear Fusion* **6** (4), 297.
- RUFFOLO, D. & MATTHAEUS, W. H. 2013 Theory of magnetic field line random walk in noisy reduced magnetohydrodynamic turbulence. *Phys. Plasmas* **20** (1), 012308.
- SAHRAOUI, F., GOLDSTEIN, M. L., BELMONT, G., CANU, P. & REZEAU, L. 2010 Three Dimensional Anisotropic k Spectra of Turbulence at Subproton Scales in the Solar Wind. *Phys. Rev. Lett.* **105** (13), 131101.
- SAHRAOUI, F., GOLDSTEIN, M. L., ROBERT, P. & KHOTYAINTEV, Y. V. 2009 Evidence of a Cascade and Dissipation of Solar-Wind Turbulence at the Electron Gyroscale. *Phys. Rev. Lett.* **102** (23), 231102.
- SAHRAOUI, F., HUANG, S. Y., BELMONT, G., GOLDSTEIN, M. L., RÉTINO, A., ROBERT, P. & DE PATOUL, J. 2013 Scaling of the Electron Dissipation Range of Solar Wind Turbulence. *Astrophys. J.* **777**, 15.
- SCHLICKSEISER, R. 1989 Cosmic-ray transport and acceleration. I - Derivation of the kinetic equation and application to cosmic rays in static cold media. II - Cosmic rays in moving cold media with application to diffusive shock wave acceleration. *Astrophys. J.* **336**, 243–293.
- SCHLICKSEISER, R. & MILLER, J. A. 1998 Quasi-linear Theory of Cosmic-Ray Transport and Acceleration: The Role of Oblique Magnetohydrodynamic Waves and Transit-Time Damping. *Astrophys. J.* **492**, 352–378.
- SERVADIO, S., MATTHAEUS, W. H., WAN, M., RUFFOLO, D., RAPPAZZO, A. F. & OUGHTON, S. 2014 Complexity and Diffusion of Magnetic Flux Surfaces in Anisotropic Turbulence. *Astrophys. J.* **785**, 56.
- SHALCHI, A. 2010a A Unified Particle Diffusion Theory for Cross-field Scattering: Subdiffusion, Recovery of Diffusion, and Diffusion in Three-dimensional Turbulence. *Astrophys. J. Lett.* **720**, L127–L130.
- SHALCHI, A. 2010b Random walk of magnetic field lines in dynamical turbulence: A field line tracing method. I. Slab turbulence. *Phys. Plasmas* **17** (8), 082902.
- SHALCHI, A. & KOLLY, A. 2013 Analytical description of field-line random walk in Goldreich-Sridhar turbulence. *Mon. Not. Roy. Astron. Soc.* **431**, 1923–1928.
- SHALCHI, A. & KOURAKIS, I. 2007a Analytical description of stochastic field-line wandering in magnetic turbulence. *Phys. Plasmas* **14** (9), 092903.
- SHALCHI, A. & KOURAKIS, I. 2007b Random walk of magnetic field-lines for different values of the energy range spectral index. *Physics of Plasmas* **14** (11), 112901.
- SHEBALIN, J. V., MATTHAEUS, W. H. & MONTGOMERY, D. 1983 Anisotropy in mhd turbulence due to a mean magnetic field. *J. Plasma Phys.* **29**, 525–547.
- SIMILON, P. L. & SUDAN, R. N. 1989 Energy dissipation of Alfvén wave packets deformed by irregular magnetic fields in solar-coronal arches. *Astrophys. J.* **336**, 442–453.
- SPATSCHEK, K. H. 2008 Aspects of stochastic transport in laboratory and astrophysical plasmas. *Plasma Phys. Con. Fus.* **50** (12), 124027.
- SRIDHAR, S. & GOLDREICH, P. 1994 Toward a theory of interstellar turbulence. 1: Weak Alfvénic turbulence. *Astrophys. J.* **432**, 612–621.
- TAYLOR, G. I. 1938 The Spectrum of Turbulence. *Proc. Roy. Soc. A* **164**, 476–490.
- TENBARGE, J. M., DAUGHTON, W., KARIMABADI, H., HOWES, G. G. & DORLAND, W. 2014 Collisionless reconnection in the large guide field regime: Gyrokinetic versus particle-in-cell simulations. *Phys. Plasmas* **21** (2), 020708.
- TENBARGE, J. M. & HOWES, G. G. 2012 Evidence of critical balance in kinetic Alfvén wave turbulence simulations. *Phys. Plasmas* **19** (5), 055901.
- TENBARGE, J. M. & HOWES, G. G. 2013 Current Sheets and Collisionless Damping in Kinetic Plasma Turbulence. *Astrophys. J. Lett.* **771**, L27.
- TENBARGE, J. M., HOWES, G. G. & DORLAND, W. 2013 Collisionless Damping at Electron Scales in Solar Wind Turbulence. *Astrophys. J.* **774**, 139.
- TENBARGE, J. M., HOWES, G. G., DORLAND, W. & HAMMETT, G. W. 2014 An oscillating Langevin antenna for driving plasma turbulence simulations. *Comp. Phys. Comm.* **185**, 578–589.

- TENBARGE, J. M., PODESTA, J. J., KLEIN, K. G. & HOWES, G. G. 2012 Interpreting Magnetic Variance Anisotropy Measurements in the Solar Wind. *Astrophys. J.* **753**, 107.
- TU, C.-Y. & MARSCH, E. 1995 MHD structures, waves and turbulence in the solar wind: Observations and theories. *Space Sci. Rev.* **73**, 1–2.
- VISHNIAC, E. T., PILLSWORTH, S., EYINK, G., KOWAL, G., LAZARIAN, A. & MURRAY, S. 2012 Reconnection current sheet structure in a turbulent medium. *Nonlin. Proc. Geophys.* **19**, 605–610.
- WANG, Y., BOLDYREV, S. & PEREZ, J. C. 2011 Residual Energy in Magnetohydrodynamic Turbulence. *Astrophys. J. Lett.* **740**, L36.
- YOUSEF, T. A., RINCON, F. & SCHEKOCIHIN, A. A. 2007 Exact scaling laws and the local structure of isotropic magnetohydrodynamic turbulence. *J. Fluid Mech.* **575**, 111.
- ZIMBARDO, G., POMMOIS, P. & VELTRI, P. 2006 Superdiffusive and Subdiffusive Transport of Energetic Particles in Solar Wind Anisotropic Magnetic Turbulence. *Astrophys. J. Lett.* **639**, L91–L94.
- ZIMBARDO, G., VELTRI, P., BASILE, G. & PRINCIPATO, S. 1995 Anomalous diffusion and Lévy random walk of magnetic field lines in three dimensional turbulence. *Phys. Plasmas* **2**, 2653–2663.
- ZIMBARDO, G., VELTRI, P. & POMMOIS, P. 2000 Anomalous, quasilinear, and percolative regimes for magnetic-field-line transport in axially symmetric turbulence. *Phys. Rev. E* **61**, 1940.
- ZWEBEN, S. J., MENYUK, C. R. & TAYLOR, R. J. 1979 Small-scale magnetic fluctuations inside the macrotor tokamak. *Phys. Rev. Lett.* **42**, 1270–1274.